JCB Journal of Cell Biology

ARTICLE

Elimination of nurse cell nuclei that shuttle into oocytes during oogenesis

Zehra Ali-Murthy[1], Richard D. Fetter[2], Wanpeng Wang[1], Bin Yang[3], Loic A. Royer[3], and Thomas B. Kornberg[1]

***Drosophila* oocytes develop together with 15 sister germline nurse cells (NCs), which pass products to the oocyte through intercellular bridges. The NCs are completely eliminated during stages 12–14, but we discovered that at stage 10B, two specific NCs fuse with the oocyte and extrude their nuclei through a channel that opens in the anterior face of the oocyte. These nuclei extinguish in the ooplasm, leaving 2 enucleated and 13 nucleated NCs. At stage 11, the cell boundaries of the oocyte are mostly restored. Oocytes in egg chambers that fail to eliminate NC nuclei at stage 10B develop with abnormal morphology. These findings show that stage 10B NCs are distinguished by position and identity, and that NC elimination proceeds in two stages: first at stage 10B and later at stages 12–14.**

Introduction

The eggs of many species are distinguished by specialized coatings, structures, and organelles that enable fertilization and early development. Another distinctive feature is the provenance of egg components, some of which are produced by the oocyte and some by other cells. The external sources in nearly all egg-laying vertebrates and invertebrates include somatic cells such as those that contribute yolk proteins. The external sources also include germline cells, whose destiny is not fertilization and zygote formation. Instead, these cells export products they make to provision a developing oocyte and, despite their germline lineage, die rather than mature to fertilization competence. *Hydra* is an example that has such sacrificial germline cells: early *Hydra* oocytes fuse with nearby germ cells that differentiate as nurse cells (NCs) and transfer cytoplasm directly to the growing oocyte (Alexandrova et al., 2005; Miller et al., 2000). Another example is the mouse oocyte, which receives cytoplasmic components including organelles such as centrioles, Golgi, and mitochondria from neighboring, interconnected sister germline cells. These nurse-like cells are eliminated by an apoptosis-like process (Lei and Spradling, 2016).

Drosophila oogenesis is arguably the system with sacrificial germline cells that is understood best. Four consecutive mitotic divisions of a primary oogonial cell generate a cyst of 16 cells in the germarium, the assembly of germline stem cells and follicle stem cells in the anterior-most region of the ovary. One of the daughters of the first division develops as the oocyte, while the other 15 descendants develop into NCs, which are considered to have equivalent function and fate. These 16 clonally related germline cells are linked by stable intercellular bridges (ring canals [RCs]) that form at sites of arrested cleavage furrows (Brown and King, 1964; Matova and Cooley, 2001). Although both the oocyte and NCs increase in volume as oogenesis proceeds, the respective developmental programs for the two cell types differ. The NCs undergo 10–12 endocycles without cytokinesis, becoming increasingly polyploid between stages 2 and 10 (for descriptive purposes, oogenesis is categorized by 14 morphologically distinct stages; Cummings and King, 1969; King et al., 1956; Spradling, 1993). In contrast, the chromosomes of the oocyte nucleus (the germinal vesicle [GV]) proceed through meiosis, and although the GV increases in size, its genome does not endoreplicate. Ooplasm constituents come from several sources, including the fat body, which secretes yolk protein that is endocytosed by the oocyte (Isasti-Sanchez et al., 2020 *Preprint*) and products that the NCs export to the oocyte through the RCs. The more posterior NC nuclei (NCN) are larger and have higher ploidy than the nuclei of more anterior NCs (Jacob and Sirlin, 1959; King et al., 1956), and there is one reported example of a gene that is expressed in some but not all NCs. In situ hybridization revealed that *idgf2* expression is enriched in two NCs that are directly next to the oocyte (Zimmerman et al., 2017).

Before stage 10, NC RNA and protein moves into the oocyte in what has been characterized as a slow, initial phase (Koch and King, 1966). Cytoplasmic flow from NCs increases the relative size of the oocyte to approximately one half the egg chamber at

[1]Cardiovascular Research Institute, University of California, San Francisco, San Francisco, CA; [2]Department of Biochemistry and Biophysics, University of California, San Francisco, San Francisco, CA; [3]Chan Zuckerberg Biohub, San Francisco, CA.

Correspondence to Thomas B. Kornberg: tkornberg@ucsf.edu.

© 2021 Ali-Murthy et al. This article is distributed under the terms of an Attribution–Noncommercial–Share Alike–No Mirror Sites license for the first six months after the publication date (see http://www.rupress.org/terms/). After six months it is available under a Creative Commons License (Attribution–Noncommercial–Share Alike 4.0 International license, as described at https://creativecommons.org/licenses/by-nc-sa/4.0/).

stage 10, and as the egg chamber grows during this period, RC diameter also increases, from ∼0.5–1.0 µm at stages 2–3 to ∼10 µm (Warn et al., 1985). The importance of RC-dependent transport is evident in *kelch* mutants, which have abnormally small egg chambers and are female sterile. Kelch protein is a structural component of RCs and is RC specific (Xue and Cooley, 1993). After stage 10, a more rapid phase of transport termed dumping depletes the NCs of their contents and increases the oocyte volume (Guild et al., 1997; Jacob and Sirlin, 1959). The NCN rearrange and congregate closely in the most anterior portion of the egg chamber, nuclear membranes disappear, and the nuclear remnants are ultimately cleared at late stage 14, leaving only the oocyte in the egg chamber. The processes that engineer NC killing and elimination have not been identified (Baum et al., 2007; Foley and Cooley, 1998; Peterson and McCall, 2013; Peterson et al., 2003).

This study describes a new feature of the NC program. We discovered that NCN are absorbed into the oocyte at late stage 10B, before the dumping phase and before the phase of nuclear condensation. This process involves fusion of the oocyte and NC plasma membranes and movement of NCN into the ooplasm. At stage 11, these NCN in the oocyte have degraded, and the plasma membranes that separate the oocyte and NCs are mostly restored. We present evidence that this unprecedented program of reversible cell fusion and nuclear elimination is essential for oocyte maturation.

Results

NCN enter the late stage 10B oocyte

The adult ovary is an assembly of ∼20 production lines (ovarioles) that each contain a string of egg chambers (King et al., 1956). Every egg chamber has 16 germline descendants of a single oogonial cell and is encapsulated by a layer of somatic follicle cells. Classification of 14 stages of oogenesis that are represented in these egg chambers is based on morphology and is not related to duration: the stages vary from 0.5 to 6 h (Dej and Spradling, 1999). Because the number of egg chambers per ovariole averages fewer than nine, not all stages are present in every ovariole or in every ovary. Checkpoints that control oocyte maturation influence the distribution of oocyte stages (Drummond-Barbosa and Spradling, 2001) and lead to over- or underrepresentation of particular stages in individual ovaries. Late stage 10B oocytes are uncommon in females raised under standard conditions of fly culture (∼0.4/ovary); we used a regimen of daily feeding that increases their frequency by ∼2.8 times to an average of 1.1 per ovary (Fig. 1 A; see Materials and methods).

We used several criteria to distinguish stage 10 egg chambers. The nucleus (GV) of stage 10A oocytes has a diameter of ∼25 µm (SD 0.8; n = 4) and localizes immediately adjacent to the anterior face of the oocyte. We visualized the GV and NCN by staining fixed preparations with α-nuclear lamin antibody and by fluorescence of GFP in nuclei of egg chambers dissected from ovaries of flies with germline expression of nuclear GFP (Fig. 1, B and B′). The GV and NCN are similar in size, but whereas most of the volume of an NC nucleus stains with DAPI, DAPI-stained DNA occupies only a small fraction of the GV. In early stage 10B, "centripetal" follicle cells begin to migrate across the anterior face of the oocyte, and the cluster of somatic "border cells" locates dorsally near the GV, which has increased in size to an ∼31-µm diameter (SD 3.0; n = 5). At late stage 10B, the GV is slightly more posterior and larger (an ∼42-mm diameter; SD 3.1; n = 5), the girth of the oocyte is increased, and the length of the oocyte relative to the NC compartment is larger. Many of these late stage 10B oocytes have ectopic nuclei that are similar in appearance to NCN: their interior is completely stained by DAPI (Fig. 1, C and D). The "ectopic" nucleus in the oocyte in Fig. 1 E was photographed while the egg chamber was incubated ex vivo, indicating that its presence is not an artifact of fixation. Evidence described in the following sections shows that these nuclei migrate into the oocyte from adjacent NCs.

Because the mitoses that generate the 16 germline cells of the egg chamber are stereotyped and are characterized by incomplete cytokinesis, the lineage of each cell is unique, and each cell is distinguished by the number of RCs that link it to its sisters (Brown and King, 1964). For example, both cells produced by the first division have four RCs, and the first daughters of these two cells each have three (Fig. 2 A). We determined the identities of the germline cells in 35 egg chambers with nuclei marked with nuclear GFP and RCs stained with α-Hts antibody. Several features are noteworthy. First, although the position of each cell was not precisely the same in every egg chamber, cells are reproducibly positioned into one of three tiers (Fig. 2, B–E). The four cells that connect directly to the oocyte (tier 1) are numbers 2, 3, 5, 9. Six cells (numbers 4, 6, 7, 10, 11, 13) are intermediate (tier 2), and five cells (numbers 8, 12, 14, 15, 16) are in the region most distant from the oocyte (tier 3). Only tier 1 cells are in direct contact with the oocyte. These results are consistent with the report of Imran Alsous et al. (2017).

Second, whereas stage 10A egg chambers have 15 nucleated NCs, most late stage 10B, stage 11, and stage 12 egg chambers have <15. Fig. 3 A is a 3D image constructed from a stack of confocal sections in which both the 15 NCN and GV of a stage 10A egg chamber are marked with GFP fluorescence. The egg chambers shown in Fig. 3, B–D, are typical of late stage 10B egg chambers in which ectopic GFP-marked nuclei are also present in the oocyte. Analysis of three genotypes (MTD-Gal4 UASp-NLSGFP, w^1, and RAL-208 WT) revealed similar frequencies of stage 10B egg chambers with entering NCN (∼0.33/ovariole) in these lines (Table S1). Among the 134 total late stage 10B oocytes with ectopic nuclei that we analyzed in the course of this work, oocytes with one ectopic nucleus in the ooplasm were most frequent (n = 93). Oocytes with two or three NCN were also observed, but they were less frequent (n = 37 and 4, respectively).

This description is based on our analysis of ovaries that were fixed immediately after removal of ovaries and before dissection of the ovary. Following fixation, ovary dissection involved teasing ovarioles apart with fine needles in ways that minimized effects on the shape or structure of the egg chambers. Although it is unlikely that the procedure used to prepare these samples forced NCN into the oocyte, we analyzed 18 stage 11 oocytes in such preparations to ensure that the presence of NCN in the stage 10B oocytes was not an artifact of preparation (Fig. 3 E).

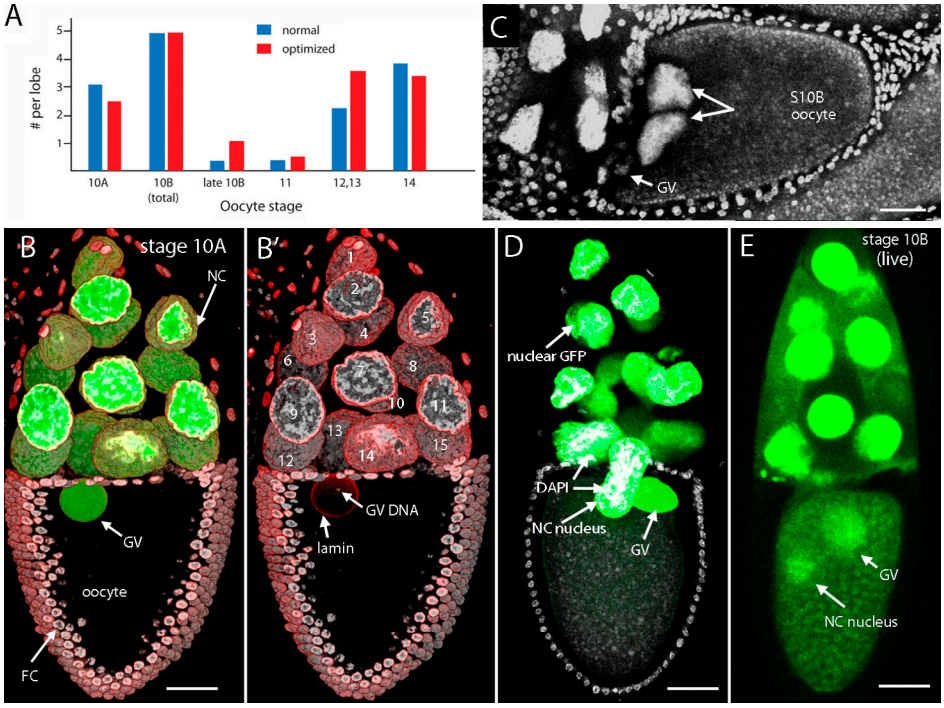

Figure 1. **NCN in stage 10 oocytes. (A)** Graph tabulating egg chamber stages in WT ovaries of females raised under normal conditions (59 ovary lobes) or conditions optimized for stages late 10B (with NCN in ooplasm) and 11 (54 ovary lobes). **(B and B′)** Stage 10A egg chambers with germline expression of nuclear GFP (green) in 15 NCN and GV, stained with α-lamin antibody (red) and DAPI (white); orientation anterior up. NC numbering: 1–15 from most anterior. **(C)** Stage 10B WT egg chamber, fixed and stained with DAPI; arrows indicate GV and NCN in ooplasm; orientation anterior left. **(D)** Fixed stage 10B egg chamber stained with DAPI (white) with germline expression of nuclear GFP, and one entering NC nucleus (arrow); orientation anterior up. **(E)** Unfixed (live) stage 10B egg chamber with germline expression of nuclear GFP (green) in 15 NCN, one in ooplasm (arrow); orientation anterior up. Scale bars: 50 µm.

Stage 11 egg chambers are infrequent, averaging <1 per 2 ovaries, but among the 18 ovaries we examined, no stage 11 egg chamber had NCN in the ooplasm, 11 (61%) had 13 nucleated NCs, and only 2 egg chambers (11%) had 15 nucleated NCs. Fig. 3, F and G, show examples of stage 11 and 12 egg chambers with 13 NCN. Videos 1 and 2 were generated from stacks of optical sections of (1) an early stage 10B egg chamber with 15 visible NCN and (2) a stage 11 egg chamber with 13 visible NCN. These results establish that the NCN in the ooplasm of late stage 10B oocytes were not induced by the procedure we used to image the preparations. We note that although approximately two thirds of egg chambers eliminate two NCN, only 28% of the oocytes we observed with ectopic NCN had more than one NC nucleus in the ooplasm. As described below, this is likely a consequence of the sequential entrances of the NCN and the rapid dissolution in the oocyte.

The reduction in number of NCN is not unique to a particular fly stock or line, but is characteristic of all the 37 WT and mutant *Drosophila melanogaster* stocks we examined. NC nuclear elimination is also a feature of *Drosophila simulans*, *Drosophila hydei*, and *Drosophila virilis* WT (Fig. 3, H–K). The images in these panels are consistent with the idea that before the onset of the program that completely clears NCs from egg chambers at stages 11–14 (Foley and Cooley, 1998), a common feature of *Drosophila* oogenesis involves the absorption of NCN into the ooplasm of late stage 10B oocytes.

To examine the process of NC nuclear elimination in more detail, we analyzed *D. melanogaster* egg chambers incubated ex vivo. Published methods support ex vivo egg chamber development to stage 9 (Prasad et al., 2007) and from stage 10B (Spracklen and Tootle, 2013), but not the period from stage 10A to stage 11, when NCN move into the ooplasm. Our observations are consistent with these reports, and an additional impediment to live imaging of nuclear elimination is the low visibility of GFP-containing nuclei deep in the ooplasm of unfixed oocytes. To circumvent these difficulties, we took advantage of our ability to identify late stage 10B oocytes using a dissecting microscope and transmitted light optics. We identified midstage 10B oocytes in ovary preparations within 10 min of dissection by the presence of a small region of ooplasmic clearing at the anterior dorsal face of the oocyte (Fig. 3 L). Viewing fixed and DAPI-stained preparations of these selected egg chambers with confocal fluorescence microscopy established that the cleared region is the GV (Fig. 3 M) that moves to this dorsal anterior location at midstage 10B (Spradling, 1993). After 10–20 min of additional incubation, a broad area of the anterior ooplasm clears (Fig. 3 N), and analysis by confocal microscopy after fixation showed that this clearing is associated with entering NCN in late stage 10B egg chambers (Fig. 3 O). The duration of clearing in 5 egg chambers that were analyzed was between 7 and 17 min (observed times: 7–10, 8–9, 8–9, 8–9, and 15–17 min), and imaging the egg chambers when the clearing was no longer visible established that these egg chambers are stage 11 and have 13 NCN (Fig. 3, P and Q). We conclude that NCN are eliminated

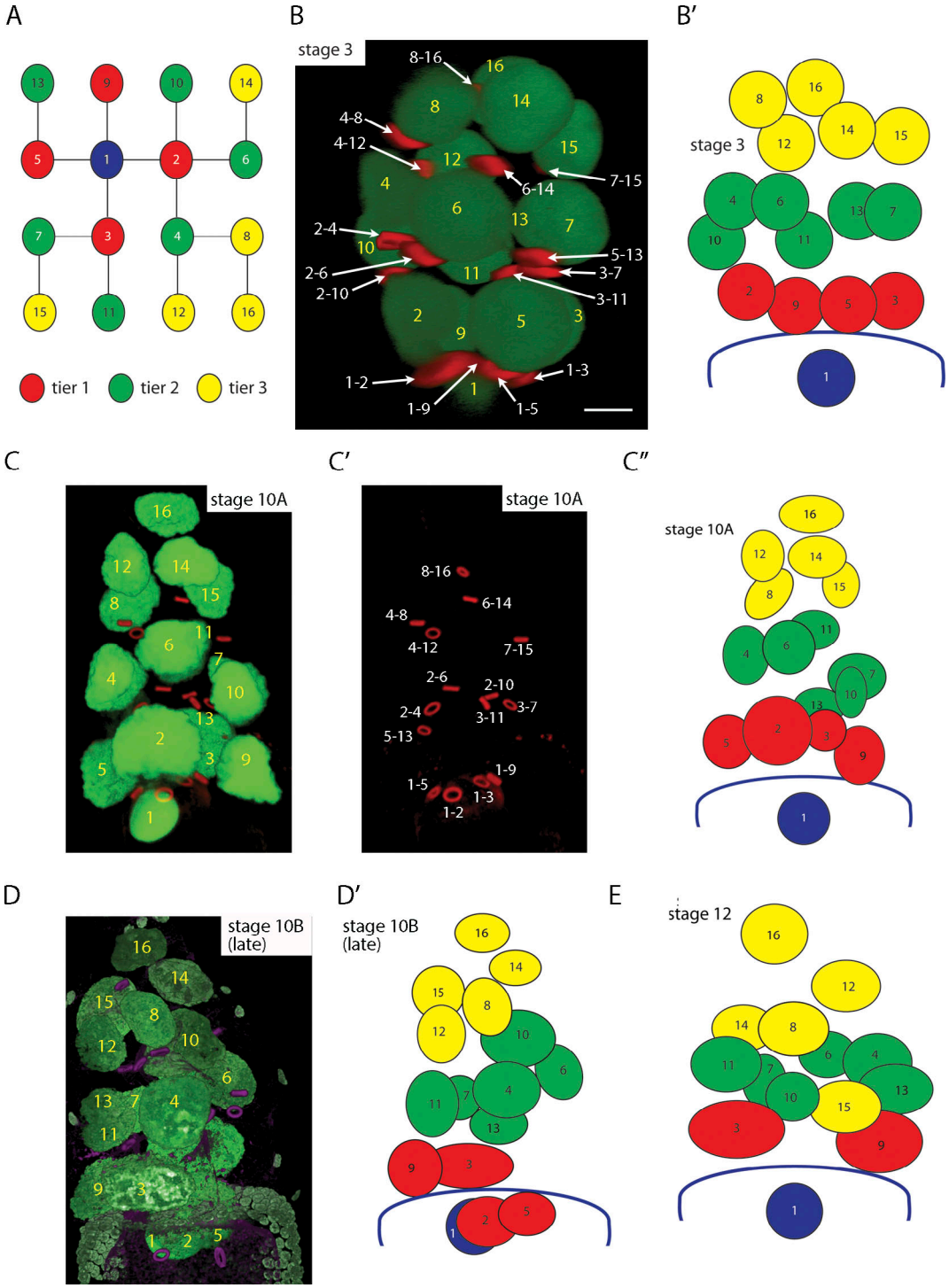

Figure 2. **Defined positions of NCN. (A)** Lineage tree of NCs; oocyte (1; blue), oocyte daughters (2, 3, 5, 9; tier 1, red), oocyte granddaughters (4, 6, 7, 10, 11, 13; tier 2, green), oocyte great-granddaughters (8, 12, 14, 15, 16; tier 3, yellow); tiers 1, 2, and 3 are touching the oocyte, in middle NC region, farthest from oocyte, respectively. **(B–E)** Orientation anterior up; number cell numbering in all panels relate to lineage indicated in A. **(B)** Stage 3 egg chamber with nuclei and RCs identities marked. **(B′)** Cartoon of egg chamber in B. **(C–C″)** Stage 10A egg chamber with identities of nuclei (C) and RCs marked (C′) and depicted in cartoon (C″). **(D and D′)** Stage 10B depicted in 3D projection (D) and cartoon (D′). **(E)** Stage 12 egg chamber depicted in cartoon. Genotype: *MTD-Gal4 UASp-nucGFP*.

within 7–17 min of their movement into the oocyte. Fig. S1 shows time-lapse fluorescence images of the early stages of NC nuclear entry captured by lattice light sheet microscopy. Video 3 was taken with transmitted light in which posteriorly moving ooplasmic clearing associated with a NC nucleus is visible.

Although the discovery of NC nuclear elimination was unexpected given the many prior published studies of *Drosophila*

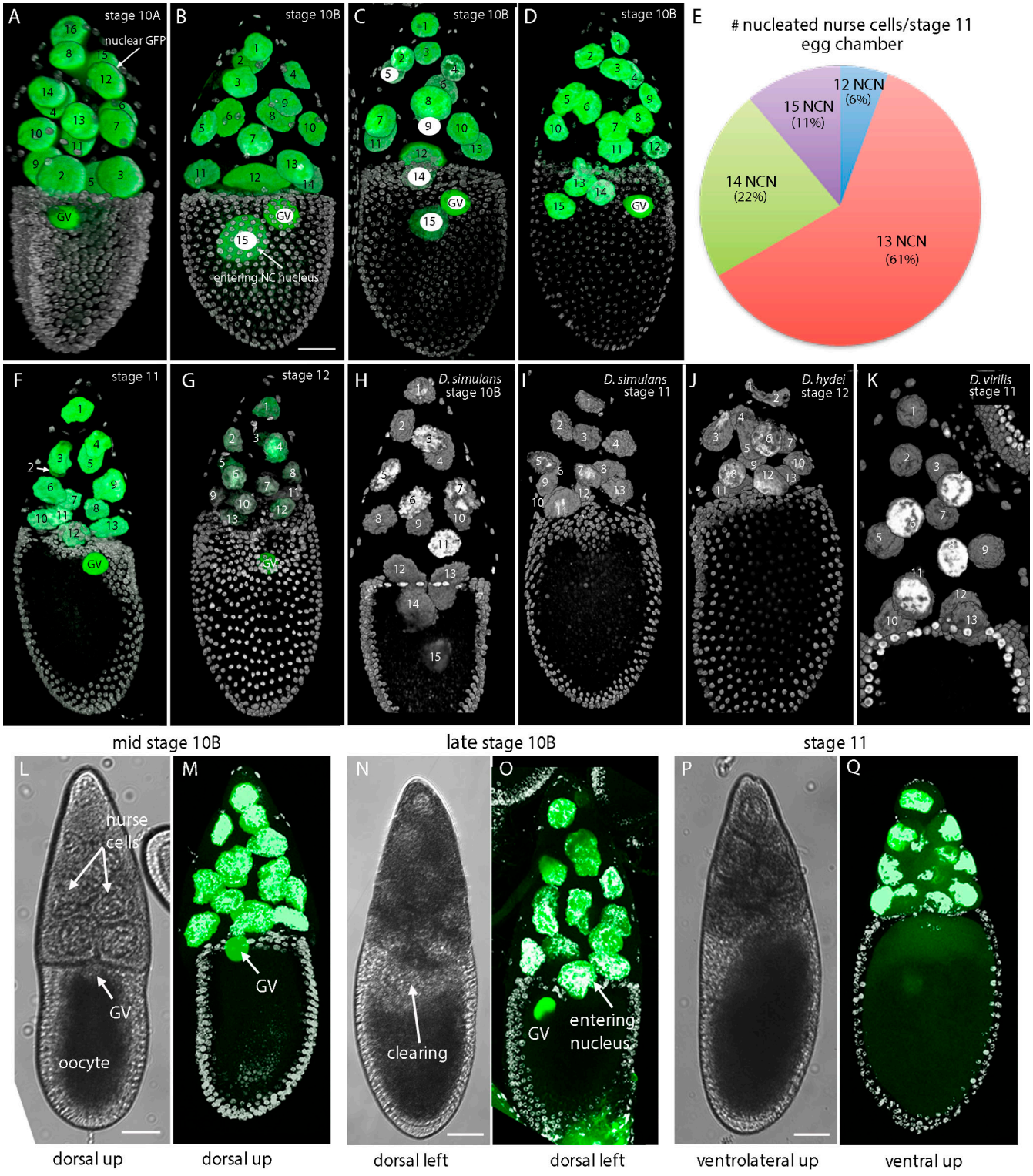

Figure 3. **NC content in *Drosophila* egg chambers. (A–G)** Analysis of *D. melanogaster* stage 10A–12 egg chambers expressing nuclear GFP (green) and stained with DAPI (white); orientation anterior up. **(A)** Stage 10A oocyte has no ectopic nuclei; numbering indicates lineage as defined in Fig. 2 A. **(B–D)** Stage 10B with one (B), two (C), or three (D) ectopic oocyte nuclei; NC numbering: 1–15 from most anterior, not according to lineage. **(E)** Pie chart indicating fraction of 18 stage 11 egg chambers that have 12, 13, 14, or 15 NCN. **(F and G)** Stage 11 (F) and stage 12 (G) egg chambers with 13 NCN and no ectopic nuclei in the oocyte. NC numbering: 1–15 from most anterior. **(H–K)** *D. simulans*, *D. hydei*, and *D. virilis* egg chambers stained with DAPI (white) with two ectopic NCN in the stage 10B *D. simulans* oocyte (H) and 13 NCN in the *D. simulans* (I), *D. hydei* (J), and *D. virilis* (K) stage 11 egg chambers. Scale bar: 50 µm. **(L–Q)** Midstage 10 (L and M), late stage 10 (N and O), and stage 11 (P and Q) egg chambers (MTD-Gal4 UASp-NLSGFP) viewed with transmitted light (L, N, and P) and fluorescence microscopy (M, O, and Q). Orientation anterior to top or figure and as indicated. Egg chambers were viewed under a dissecting microscope during ex vivo incubation and distinguished both by relative size of the oocyte and by opacity of anterior ooplasm for identification of GV at midstage 10 (L), entering NCN at late stage 10B

(N), and stage 11 (P). Egg chambers were photographed at the three indicated stages or were fixed, stained with DAPI, and mounted for imaging with a confocal microscope. Timing was ≤10 min after isolation (L and M), 10–20 min after appearance of GV at anterior oocyte membrane (N and O), and 7–17 min after appearance of broad anterior clearing (P and Q). Scale bars: 50 µm.

oogenesis that did not describe either these ectopic nuclei or the reduction in NCN, there are several published descriptions that are consistent with our findings and are cited in the Discussion. It was our ability to highlight the key structures with bright fluorescent markers and analyze many egg chambers in 3D that made our observations and conclusions definitive.

To determine if the nuclei that enter the oocyte are a random selection from the 15 NCs or are from particular NCs, we ascertained the identity of all nucleated NCs in 20 stage 10 egg chambers. Two were stage 10A and eight were early 10B; none of the oocytes had entering NCN. In contrast, the 10 oocytes of mid- and late stage 10B egg chambers had entering NCN from NCs 2 (the sister of the first mitotic division) and 5 (the sister of the third mitotic division; Fig. 2 A and Fig. 4, A and A′). Both cells 2 and 5 are tier 1 cells and are directly linked to the oocyte by RCs. In 7 of the 10 late stage 10B egg chambers, the nucleus from NC2 is entirely within the ooplasm and only a portion of the NC5 nucleus is within the ooplasm; in 3, both NC2 and NC5 nuclei are entirely in the ooplasm. These findings reveal that the process of nuclear migration is specific to particular NCs and that the NC2 nucleus is the first to enter and suggest that at least two of the NCs in each stage 10B egg chamber may be different from the others.

The four tier-1 NCs are direct descendants of the oocyte, and each tier-1 cell connects directly to the oocyte through an RC. At stage 9, the four RCs are evenly spaced on the anterior face of the oocyte, and each RC is located within a quadrant of a planar, circular structure that is visible after cadherin and phalloidin staining (Fig. 4, B–D). These images show that the anterior face of the oocyte is continuous at stage 9. However, this quadrant structure of RCs is temporary. Whereas cadherin and phalloidin staining is uniform across the NC:oocyte interface at stage 9, staining is not continuous at stage 10: gaps are present at NCs 2 and 5 (Fig. 4 E), and the RCs that join the oocyte to NCs 2 and 5 (RC1–2 and RC1–5) are posterior to the plane of the oocyte anterior face (Fig. 4 A). RC1–2 and RC1–5 are in the interior of the oocyte and appear to precede the entering NCs 2 and 5 that are nearby. We observed 26 oocytes with entering NCN in this study, and all had RCs in the oocyte posterior to the entering nuclei. 19 of the oocytes had 1 entering nucleus and 1 RC; 7 had 2 entering nuclei and 2 RCs. The RCs were small relative to entering NCN (diameter ∼14 vs. ∼44 µm), and because the fluorescent images are not consistent with a direct association between the NCN and RCs, we conclude that the NCN do not extrude through the RCs. At stage 11, RC1–2 and RC1–5 are again located at the anterior planar interface of the oocyte and are again organized in an evenly spaced pattern (Fig. 4, F–G′). A previous report (Warn et al., 1985) noted RCs in the ooplasm of stage 10 oocytes as "unpublished observations."

In our stage 10B preparations, the fluorescence of nuclear GFP revealed the locations of NCN 2 and 5, but the images did not distinguish whether the nuclei are expelled from the NCs or the NCs are engulfed by the oocyte in their entirety. We did not have a way to independently mark NCs 2 and 5, but three observations are consistent with the idea that NCs 2 and 5 remain in their original location. First, whereas RC1–2 and RC1–5 (which connect NCs 2 and 5 with the oocyte) move into the oocyte together with the entering NCN, RC2–4, RC2–6, RC2–10, and RC5–13 did not appear to change their relative location (Fig. 4, A and A′). This is consistent with the idea that the morphologies of NCs 2 and 5 at the contacts with NCs 4, 6, 10, and 13 did not change. Second, the process of nuclear extrusion appears to have left NCs 2 and 5 as enucleated structures at stage 11, and the adjoining cells did not expand into the spaces that the nuclei of NCs 2 and 5 vacated at stage 10B. These spaces were devoid of nuclei in stage 10B egg chambers with entering NCN (Fig. 5, A and B) and stage 11 egg chambers (Fig. 5 C).

Third, NCs 2 and 5 are large, and their movement into the oocyte might be expected to increase the volume of the oocyte when they enter. We measured the volumes of egg chambers and oocytes from stage 2 to stage 13 and determined that the egg chamber volume and oocyte volume increased with average doubling times of 6.7 and 5.5 h, respectively (Fig. 5 D and Table S1). As noted in previous studies, however, a rapid phase of "terminal injection" during the stage 10B to stage 14 period increases oocyte volume more rapidly, when dumping moves all the contents of NCs into the oocyte (Guild et al., 1997; Jacob and Sirlin, 1959). The oocyte doubling time we measured was 5.9 h for stages 2–11 and 2.8 h for stages 11–13, but our analysis of stage 10–11 egg chambers did not detect a significant change in the growth rate of the oocyte specifically at stage 10B, when the nuclei of NCs 2 and 5 enter the oocyte.

A channel connects the oocyte and NCs at stage 10B

We investigated how the NCN might enter the late stage 10B oocyte by using various markers to examine the distributions of NCN, RCs, and GV with respect to the plasma membranes of follicle cells, border cells, and oocyte (Fig. 6, A–F). In the four egg chambers imaged in these panels, the proximity and relative positions of the GV (Fig. 6, A–C) and border cells (Fig. 6, D and F) are typical, and the images are representative of our attempts to detect cell plasma membranes in the region where the NCN enter the oocyte. Phalloidin and cadherin staining and fluorescence of membrane-tethered GFP delineated plasma membrane of the follicle cells and oocyte in lateral regions but not in the immediate region of the entering NCN. Dpp:Cherry fluorescence that is prominent in the centripetal cells was also absent from this region (Fig. 6, E and F). The apparent absence of plasma membrane in these images contrasts with similar images of stages 9 and 11 egg chambers that show phalloidin and cadherin over the anterior oocyte face (Figs. 4 and 5). Although these results are consistent with the idea that plasma membranes in this region of late stage 10B egg chambers do not separate the oocyte from NCs, we could not rule out the possibility that confocal fluorescence imaging had insufficient sensitivity to

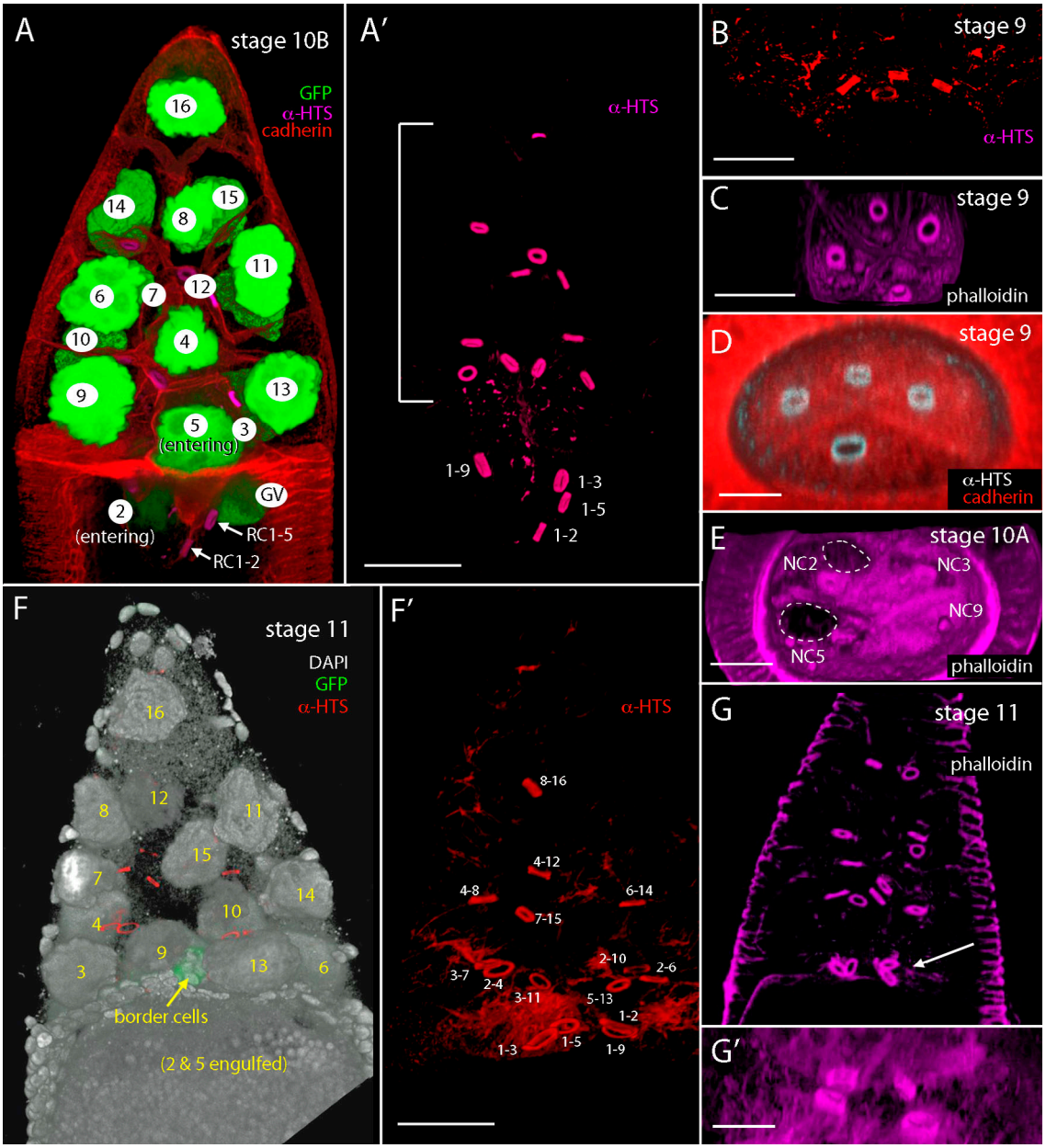

Figure 4. **Ring canals precede NCN into oocyte. (A and A′)** Stage 10B egg chamber expressing nuclear GFP (green), stained with α-HTS antibody to mark RCs and α-cadherin antibody to mark cell boundaries, with nuclei identified. Ring canals linking oocyte with NC 2 (RC1–2) and NC 5 (RC1–5) are positioned in the oocyte posterior to the entering nuclei of NCs 2 and 5; other RCs are bracketed; orientation anterior up. **(B–E)** Transverse sections created from 3D projections of confocal optical sections to show arrangements of RCs (marked with α-HTS antibody [B and D] or phalloidin fluorescence [C and E]) at the anterior face of stage 9 and stage 10 oocytes. **(E)** Gaps in fluorescence-marked anterior oocyte face are at sites of NCs 2 and 5 (dashed boundaries). **(F and F′)** Stage 11 egg chamber lacks NC 2 and 5 nuclei; stained with DAPI (white) and with α-HTS antibody to mark RCs, all of which are anterior to the oocyte; nuclear GFP marks border cells (green; 3745-Gal4); orientation anterior up. **(G)** RCs marked with phalloidin staining in stage 11 egg chamber, with four RCs at the anterior oocyte face (arrow); orientation anterior up. **(G′)** Higher-magnification image of region with four oocyte-linked RCs. Scale bars: 50 mm.

detect membranes in this region. We therefore obtained high-resolution images by EM.

We selected stage 10B egg chambers with entering NCN using a dissecting microscope equipped with transmitted light to identify oocytes with anterior regions that were slightly cleared. These egg chambers were placed immediately and directly in fixative and processed for EM. The six sections in Fig. 6 G show a stage 10B egg chamber at 10-µm intervals. Whereas the continuity of the membrane across the anterior face of the oocyte is evident in sections 1 and 6, the intermediate sections 2–5 do not have plasma membrane in the region of the entering NC nucleus. Instead, the central region of the anterior end of the oocyte connects oocyte and NC cytoplasm directly. A NC nucleus spans this apparent channel.

To address the possibility that the plasma membranes that separate the oocyte from the NCs in this region at earlier stages

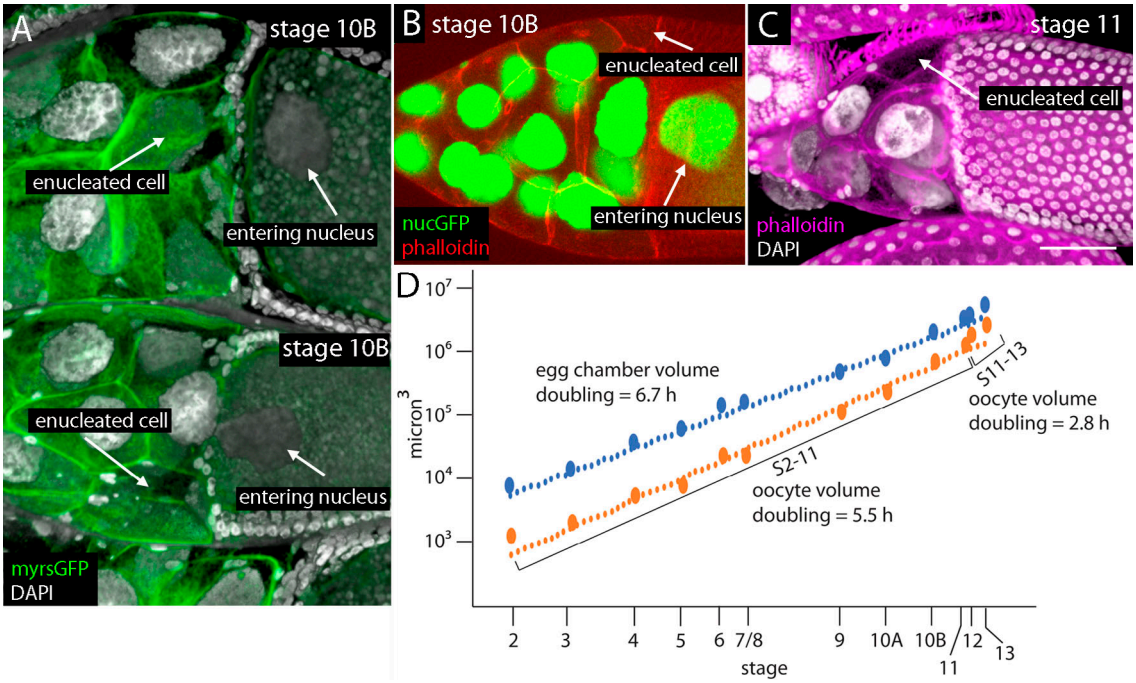

Figure 5. **Enucleated NCs in stage 10B and stage 11 egg chambers. (A and B)** Enucleated NCs indicated (arrows) in stage 10B chambers expressing myristoylated-GFP and stained with DAPI (A) or expressing nuclear-GFP and stained with phalloidin (B). **(C)** Enucleated NC of stage 11 egg chamber stained with phalloidin and DAPI. **(D)** Graph showing volumes of stage 2–13 egg chambers (80 egg chambers analyzed; data in Table S2). Scale bar: 50 µm for A–C.

are displaced posteriorly at late stage 10B, a central column of the entire length of a stage 10B oocyte was imaged at high magnification, and a montage was assembled (Fig. S2, A and B). An entering NC nucleus is visible at the most anterior end of the column, and its nuclear membrane is clearly delineated (Fig. S2 C). At the posterior end of the column, the plasma membrane of the oocyte is visible at the interface with vitelline membrane material that is interposed between the oocyte and follicle cells (Fig. S2 D). No plasma membrane is visible in the images of the ooplasm between the NC nucleus and the posterior end of the oocyte (Fig. S2 B). We conclude that plasma membranes do not separate the oocyte and NCs at late stage 10B and that NCN enter the oocyte through a channel that connects the oocyte and NCs. The morphology of this egg chamber is therefore consistent with the idea that cytoplasm of the oocyte and NCs is continuous and that the plasma membranes in this region have rearranged.

Membrane fusion joins the oocyte and NCs

The presence of a channel at the anterior face of the oocyte requires a structural rearrangement of the oocyte and NC plasma membranes. To examine the nature of this novel transition, and to determine whether the oocyte and NCs have separate and independent openings or the oocyte and NC membranes fuse, we analyzed the edge of the opening in high-resolution images such as those shown in Fig. 7. An NC nucleus extends posteriorly into the oocyte in the space that has follicle cells on both sides (Fig. 7 A). Our interpretation of the membrane profiles in the region bounded by the red dashed lines is shown in Fig. 7 B: (1) the blue lines trace deep indentations of the NC nuclear membrane, including cross sections through portions of the convoluted nuclear surface which appear detached in this section; (2) the green lines trace the plasma membranes of follicle cells on the left side of the channel; and (3) the red line traces the plasma membranes of the oocyte and NC. The high-magnification images in Fig. 7, C and D, show that the plasma membranes of the oocyte and NC are continuous. The oocyte plasma membrane extends around the dense material of the vitelline membrane at the edge of the channel and around the finger-like protrusion of a follicle cell, connecting directly with the plasma membrane of the NC that extends anteriorly and is juxtaposed with follicle cell plasma membranes. These images are consistent with the idea that the plasma membranes of the oocyte and NCs fuse to create a channel that directly connects oocyte and NC cytoplasm.

Structure and fate of the entering NCN

We characterized the constitution of entering NCN, which change shape in stage 10B egg chambers as they extrude into the oocyte (Figs. 1, 3, 6, and 7). Entering nuclei in the oocyte:NC channel had an elongated, dumbbell-like shape (Fig. 1 D; and Fig. 8, A–A‴) that is similar to the shape of the entering nucleus visible in the video obtained by light sheet microscopy (Video 2). Although actin cables are prominent in other stage 10B NCs (Huelsmann et al., 2013), phalloidin staining did not detect actin cables in or around entering NCN (Fig. 8 A″), and the uniform distributions of nuclear DNA and GFP are consistent with the idea that nuclear contents are not reorganized or condensed during extrusion through the NC:oocyte channel. Staining for nuclear membrane markers such as Msp300 and lamin (Fig. 8, B and B′) and fine-structure analysis (Fig. 8, C and C′) similarly revealed no apparent change to the nuclear membranes of the

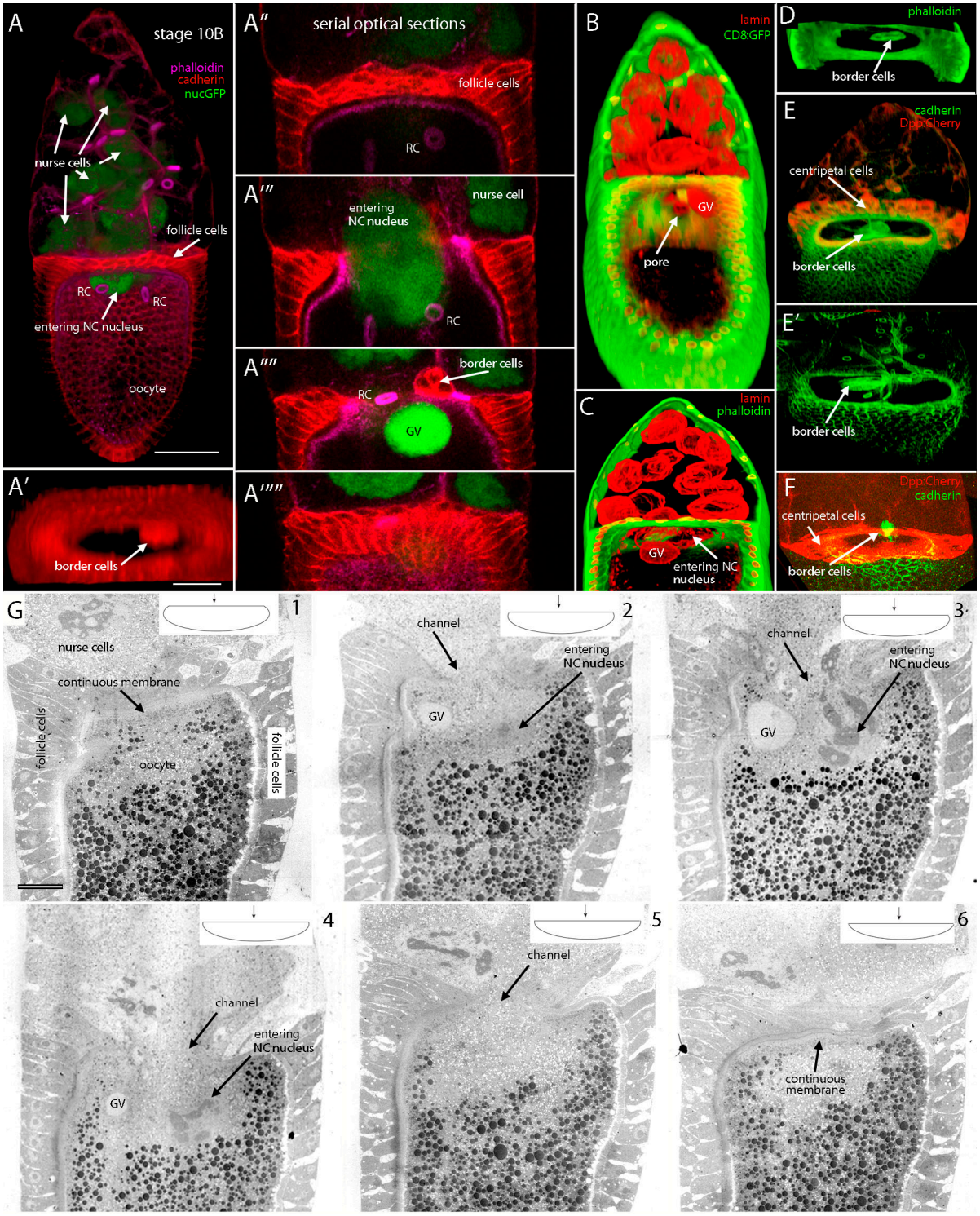

Figure 6. **Anatomy of the anterior face of the stage 10B oocyte. (A–A⁗′)** Stage 10B egg chamber marked with nuclear GFP (green), phalloidin fluorescence (purple), and α-cadherin staining (red) identifies oocyte, NCs, NCN, follicle cells, border cells, and RCs, but phalloidin or cadherin staining is absent at the anterior face of the oocyte at the site of entering NC nucleus. Frontal optical sections, orientation anterior up (A and A″–A⁗′) and transverse section created from a 3D projection of confocal optical sections (A′). **(B–F)** 3D projection images of stage 10B egg chambers with channel at oocyte anterior face, rotated for partially axial orientations, marked with membrane-tethered GFP (green) and α-lamin (red; B), α-lamin (red) and phalloidin fluorescence (C), phalloidin fluorescence (D), and Dpp:Cherry (red) and α-cadherin (green; E, E′, and F). Arrow indicates channel (B). **(G)** EM images of successive sections of a stage 10B oocyte showing continuous plasma membrane across the anterior oocyte face (1 and 6) and channel through which a NC nucleus enters (2–5). Orientation anterior up (B, C, and G). Cartoons depict sectioned egg chamber. Scale bars: 50 µm (bar in A for A–D and F; bar in A′ for A′–A⁗′, E, and E′); 20 µm (G).

entering nuclei. However, mAb414, which recognizes four nucleoporin proteins of the nuclear pore complex (Davis and Blobel, 1986; Meier et al., 1995), did not stain the entering NCN at the same level as it stained the other NCN (Fig. 8 A‴). In all 13 egg chambers stained with mAB414 that had entering NCN, the portion of the NC nuclear membrane that was inside the oocyte stained either at reduced levels or levels that were not detected. We infer that the molecular constitution of the nuclear envelope might change upon entering the oocyte.

NCN that were deep in the oocyte interior were not round spheres and were larger than other NCN (Figs. 1 and 3), and fluorescence of DAPI and nuclear GFP was low and diffuse (Fig. 8, D and D′) relative to nuclei in nucleated NCs (Figs. 1, 2, 3, 4, and 5). The NCN in the oocyte disappear, but we were not able to determine how they are eliminated. Previous studies of NC elimination at later stages (Peterson and McCall, 2013) have not determined whether it is apoptotic or autophagic, and we did not observe that the entering NCN stain with α-DCP-1 antibody.

The oocyte:NC interface of stage 11 egg chambers

To our knowledge, the scale of the membrane fusion between the oocyte and NCs is unprecedented. It is also, apparently, mostly reversible. The RCs that precede the NCN into the oocyte appear to return to their original positions at stage 11, reforming the patterned quartet of RCs set in the membranes at the NC:oocyte interface (Fig. 4, G and G′). This finding suggests that the channel that directly connects the oocyte and NCs at stage 10B closes at stage 11. To characterize the interface of oocytes and NCs at stage 11, we therefore examined EM sections of a stage 11 egg chamber and found that although the egg chamber does not have a large channel at the oocyte–NC interface, and although the vitelline membrane and follicle cells extend across the anterior face of the oocyte, a small gap remains (Fig. 8, E–H). We also examined preparations of stage 11 egg chambers by confocal fluorescence microscopy but were not able to resolve the separate plasma membranes of the oocyte and NCs in this morphologically complex region (Fig. S3). These results are consistent with the idea that the channel does not completely close and that there is continuity between ooplasm and enucleated NCs in stage 11 egg chambers.

NC nuclear elimination is essential for oocyte maturation

Counts of NCN in stage 11 egg chambers (Fig. 3 E) show that ∼90% had <15 NCN and ∼10% did not reduce the number of NCN. We analyzed stage 11–14 egg chambers in WT ovaries to investigate whether the process of nuclear elimination is necessary for egg chamber development. The total number of NCN was determined in fixed and DAPI-stained stage 11, 12, and 13 egg chambers that also expressed nuclear-localized GFP. Fig. 9 A shows a typical stage 12 egg chamber, identified by the length of the oocyte, area and cell density of NC region, and appearance of indentations and follicle cell patterns that mark the initiation of dorsal appendage development. This egg chamber has 13 NCN. In contrast, the stage 12 egg chamber shown in Fig. 10 B has 15 NCN, and the distance between the dorsal appendage indentations (83 µm) is greater than the interappendage distance (58 µm) of the egg chamber shown in Fig. 9 A. Stage 13 egg chambers were identified by the presence of dorsal projections that extend from the indentations. Stage 13 egg chambers with 15 NCN were distinguished from the egg chamber with 13 NCN by the greater distance between the dorsal appendage primordia (75 µm vs. 38 µm) and by the less compacted distribution of NCN (Fig. 9, C and D). All egg chambers we identified with this morphology (n = 51) had 15 NCN, and although the spacing between the dorsal appendage primordia decreased as egg chambers matured, the difference between the egg chambers with 13 or 15 NCN was consistent among all that we analyzed (Fig. 9 E).

Stage 14 egg chambers do not contain NCs or NCN, but we identified two distinct morphologies in WT ovarioles. Most stage 14 egg chambers had the expected, normal appearance of the one imaged in Fig. 9 F, but some had distinct abnormalities that included dorsal appendages that are misshaped and are spaced at a greater distance than normal (Fig. 9, E and G). Because the peculiarities of these abnormal stage 14 oocytes may be related to the abnormalities we identified in earlier-stage egg chambers that have 15 NCN, we imaged live stage 12–13 egg chambers under transmitted light and identified egg chambers with either normal or abnormal morphology. Representatives of the two classes were fixed, and examination using confocal microscopy confirmed that normal morphology was associated with 13 NCN and abnormal morphology was associated with 15 NCN. Four with abnormal morphology and five with normal morphology were incubated and allowed to develop ex vivo to stage 14 (Fig. 9, H–K). Five of five with normal morphology at stage 12–13 developed to stage 14 with normal morphology, and four of four with abnormal morphology at stage 12–13 developed to stage 14 with morphology similar to the oocyte in Fig. 9 G. These findings are consistent with the idea that the abnormal stage 14 oocytes developed from egg chambers that did not complete nuclear elimination.

To gauge whether the abnormal stage 14 oocytes might inhibit egg laying, we compared the frequency of abnormal stage 11–13 and stage 14 oocytes for females aged 3 and 10 d after eclosion. As shown in Fig. S4 A, the frequency of abnormal oocytes increased with age, the frequencies of abnormal stage 11–13 and stage 14 oocytes increased to similar extents (3.2× and 4.1×, respectively), and the ratio of abnormal stage 11–13 and stage 14 oocytes (2.1 and 1.7, respectively) were similar at 3 and 10 d. These ratios are consistent with the idea that the abnormal stage 14 oocytes were laid at normal rates and were not retained.

To determine the fate of the abnormal stage 14 oocytes, we examined the morphologies of embryos that failed to develop, because we did not expect eggs with misshapen anterior regions to be fertilized. Eggs deposited by WT females were collected and aged for 24 h. We first collected eggs from WT females of indeterminate (mixed) age and found that ∼90% developed to the first-instar larval stage and hatched. This is the expected proportion, but examination of the nonviable eggs revealed that approximately half had normal morphology, and the presence of internal organs suggested that they had been fertilized (Fig. S4, A and C). The remaining undeveloped eggs had abnormal dorsal appendages (Fig. S4 B), and the absence of internal organs suggested that they had not been fertilized (Fig. S4 D). The shapes of these eggs varied, as shown in the two examples

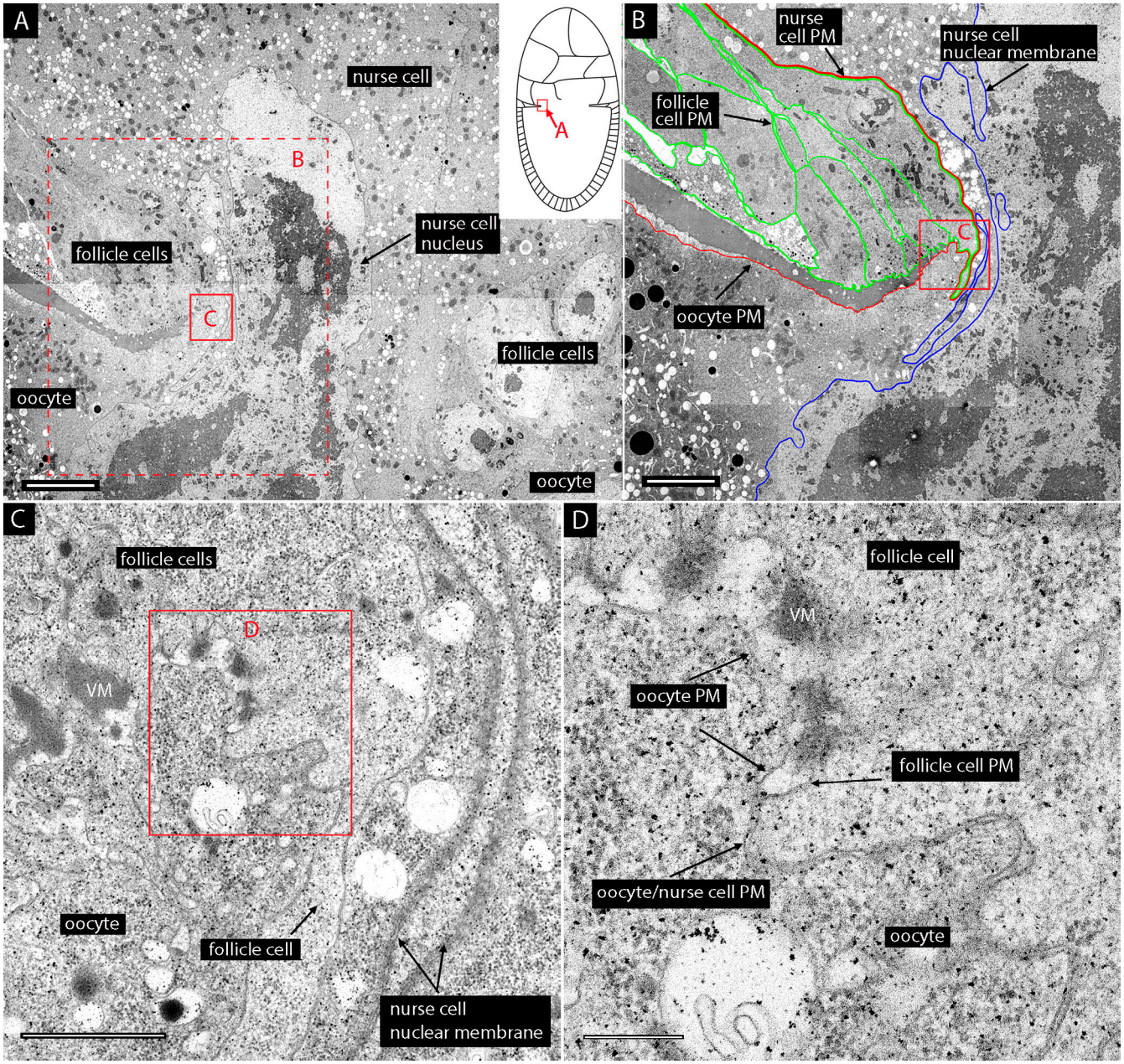

Figure 7. **Contiguous plasma membrane of the oocyte and NC. (A)** EM of an entering NC nucleus. Cartoon indicates position in egg chamber. **(B)** Dashed red-lined box in A imaged at higher magnification with traced plasma membranes (PM) of follicle cells (green), contiguous plasma membranes of oocyte and NC (red), and nuclear membrane of entering NC (blue). **(C)** Red-lined box in B imaged at higher magnification. **(D)** Red-lined box in C imaged at higher magnification. Scale bars: 5 µm (A and B); 1 µm (C); 0.25 µm (D).

provided. 3-d-old females laid fewer eggs with abnormal morphology (2.5%) than did older 10-d-old females (12.7%). These proportions of morphologically abnormal, infertile eggs were the same as the proportions of abnormal stage 14 oocytes in the ovaries of these animals (Fig. S4 A). Based on the fact that the distinctive morphology of these eggs (abnormal size and dorsal appendage spacing) is similar to the morphology of abnormal stage 14 oocytes, and based on the similar proportions of morphologically abnormal oocytes and abnormal eggs, we suggest that the abnormal unfertilized eggs may develop from the morphologically abnormal stage 14 oocytes.

Discussion

The separate fates of the *Drosophila* oocyte and 15 sacrificial NCs are set at the first division of the primary oogonial cell (de Cuevas and Spradling, 1998). The NCs form a syncytium connected by intercellular bridges, appearing to function as a single unit dedicated solely to provisioning the oocyte. Unexpectedly, we found that two particular NCs are enucleated before the onset of programmed NC death in an elaborate process (summarized in Fig. 10) that involves fusion of the NCs with the oocyte, extrusion of the nuclei into the oocyte, and degradation of the nuclei. Enucleation of these two NCs is evidence that all

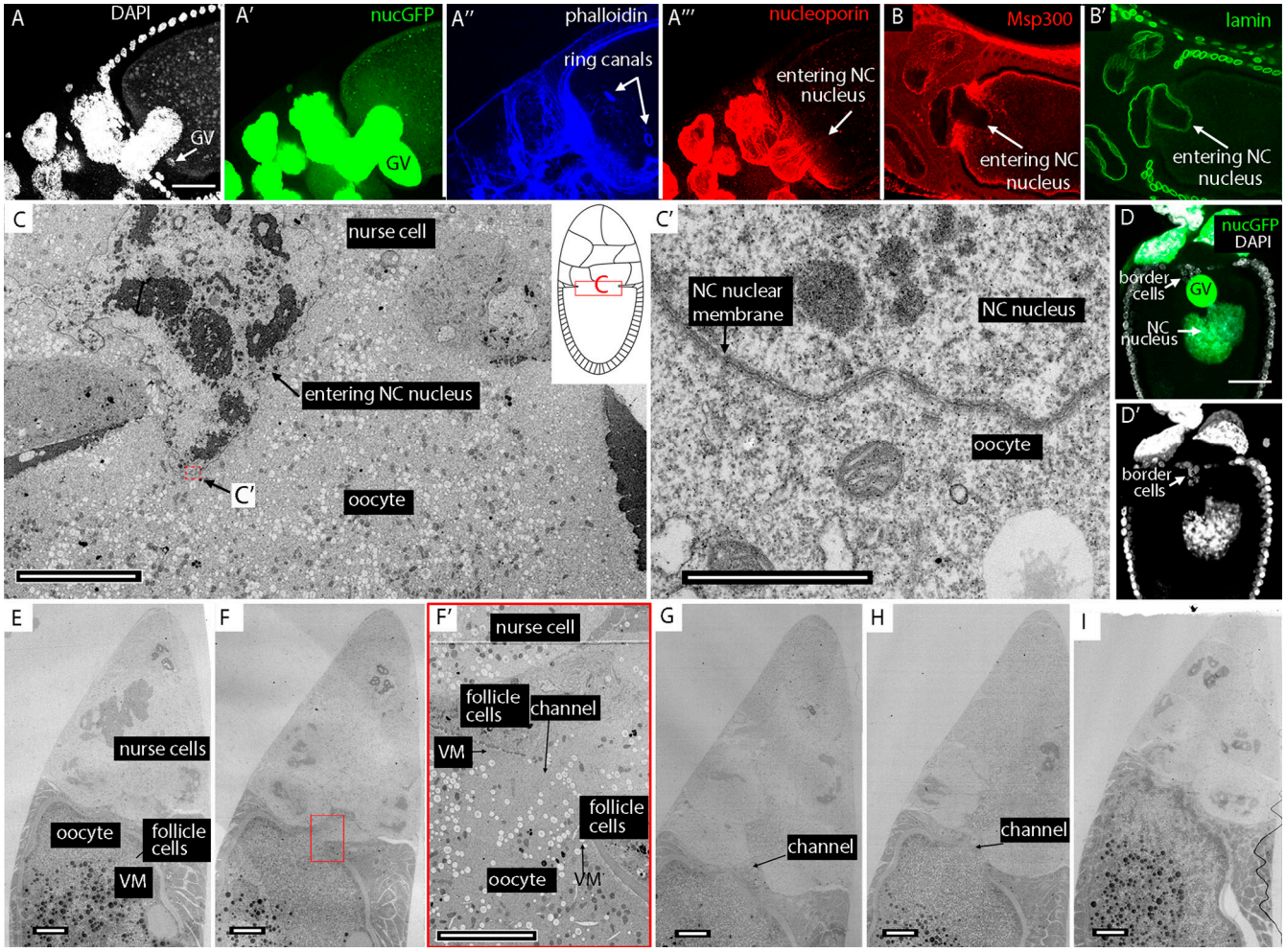

Figure 8. **Anatomy of the nuclear membrane of the entering NC nucleus and fine structure of anterior face of a stage 11 oocyte. (A–A‴)** The entering NC nucleus of the stage 10B oocyte is imaged with DAPI (white, A), nuclear GFP (green, A′), phalloidin (blue, A″), and α-nucleoporin, which stains only the portion of the nucleus that has not entered (A‴). **(B and B′)** Entering NC nucleus stained with α-Msp300 (red) and α-lamin (green) antibodies. **(C)** EM of entering NC nucleus (position in egg chamber indicated by cartoon) with red-lined region shown at high magnification in C′. **(D and D′)** Nuclear GFP (green) and DAPI (white) marks NC nucleus in the ooplasm, border cells, and GV. **(E–I)** Successive sections imaged by electron microscopy of a stage 11 egg chamber showing contiguous plasma membrane at the anterior oocyte face in outer sections (E and I) and channel in intermediate sections (F–H). **(F′)** Higher-magnification image of red-lined boxed region in F showing NC, follicle cells, vitelline membrane (VM), oocyte, and channel. Scale bars: 50 µm (bar in A for A–B′, bar in D for D and D′); 20 µm (E–I); 10 µm (C); 1 µm (C′); 10 µm (F′).

NCs do not follow the same developmental program. The abnormality of oocytes that do not successfully execute the enucleation program suggests its importance.

The first issue we address is the novelty of our findings for a system that has been so thoroughly studied for >60 yr. If NCN extruding into the oocyte are so obvious in the images we obtained, then it is important to know that these structures cannot be attributed to some aspects of the flies we studied or to the particular methods we used. The studies described in this paper investigated the process of enucleation over a span of >4 yr in >140 different *D. melanogaster* lines, which included some that had been cultured in the laboratory for many years as well as some more recently obtained from stock centers. Some had been treated with antibiotics to eradicate *Wolbachia*. The enucleation process was observed in all the lines we examined. Because enucleation was also observed in three other *Drosophila* species, we are confident that NC nuclear elimination is not unique to particular lines.

To address the concern that the method we used to isolate the egg chambers might induce the movement of NCN into the oocyte at stage 10B—that, for example, enucleation might be an artifact caused by pressure during the dissections—we analyzed WT stages 11 and 12 egg chambers that were fixed immediately after removal from the female and before dissection of the ovary. Stages 11 and 12 oocytes in these preparations had developed through stage 10B in vivo before removal and dissection, but not one had an ectopic NC nucleus. Because the time from beginning of stage 10B to stage 12 is 4.5 h, the fact that ∼90% of stage 11–12 egg chambers had <15 NCN (Fig. 3 E) is compelling evidence that the method of preparation we used did not induce enucleation.

The question remains why the ectopic NCN and their precocious elimination had not been analyzed previously. Part of

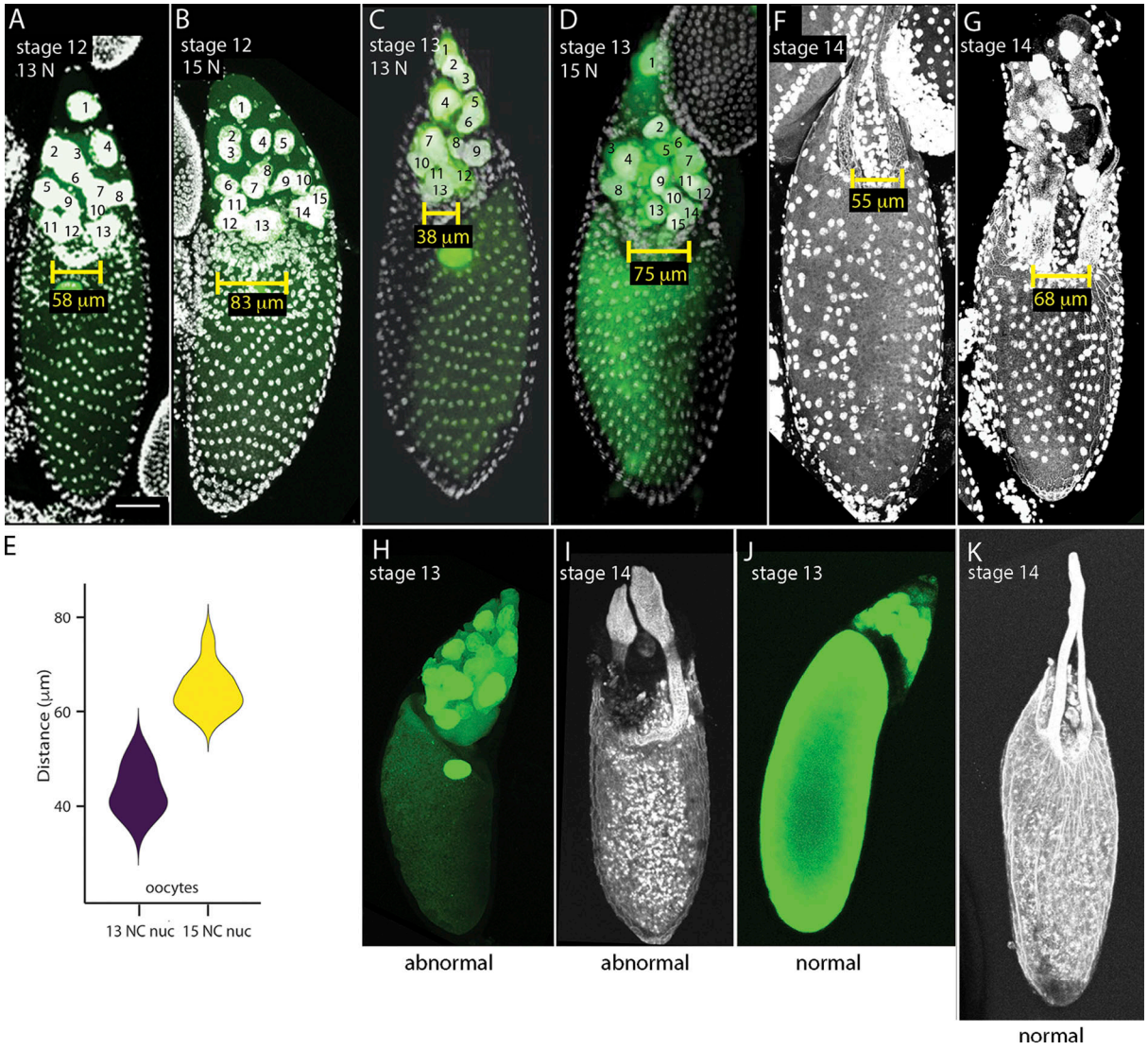

Figure 9. **Abnormalities of egg chambers that do not eliminate NCN. (A–D)** Stage 12 (A and B) and stage 13 (C and D)egg chambers marked with nuclear GFP fluorescence (green) and stained with DAPI (white) with 13 (A and C) and 15 (B and D) NCN, respectively, with distance between developing dorsal appendages marked. **(E)** Violin plot showing distributions of distances between dorsal appendages of stage 12/13 oocytes with either 13 or 15 NCN (NC nuc). **(F and G)** Stage 14 egg chambers with normal (F) and abnormal morphology (G). **(H–K)** Egg chambers (MTD-Gal4 UASp-NLSGFP, DAPI) identified at stage 13 as morphologically abnormal (H) or normal (J) and then fixed for imaging, or cultured for 5+ h at RT after morphological characterization as abnormal (I) or normal (K). Scale bar: 50 µm (bar in A for A–D and F–K).

the reason may be the greater sensitivity and resolution that is now possible with contemporary microscopes, software programs for viewing images, fluorescent molecules, and techniques for expressing marked proteins. These technical advances may have provided us with superior ways to image the preparations, but there are, in fact, results described in prior studies that are consistent with our conclusions. First, one of the features of NC movement into the oocyte that we noted is the presence of RCs that precede the nuclei into the oocyte and appear to "float" in the ooplasm (Fig. 4 A). Warn et al. (1985) make the following statement: "Several egg chambers were also found with isolated rings detached from any plasmalemma. Usually they were present inside the oocyte (not shown)." Second, the autoradiography study of Jacob and Sirlin (1959) describes a section of a stage 10 egg chamber as follows: "A stage 10 chamber... Cytoplasm from the nurse cells flows into the growing oocyte through the gap in the epithelial wall." We suggest that this gap is the channel that forms when NCs fuse with the oocyte (Figs. 6 and 7). Third, the analysis of DNA synthesis reported by Jacob and Sirlin (1959) led to the conclusion that "the trophocytes [NCs] adjacent to the oocyte have larger nuclei, and their chromosomes undergo one more replication than the anterior (distal) trophocytes. These cells subsequently lose their DNA, but the anterior cells do not" (Chapman, 1999). These observations are consistent with our finding that the two most posterior NCN are eliminated at stage 10B. Fourth, Fig. 1 in Cummings and King (1970) clearly depicts a channel that directly connects NCs with the oocyte in a stage 12 egg chamber. Fifth,

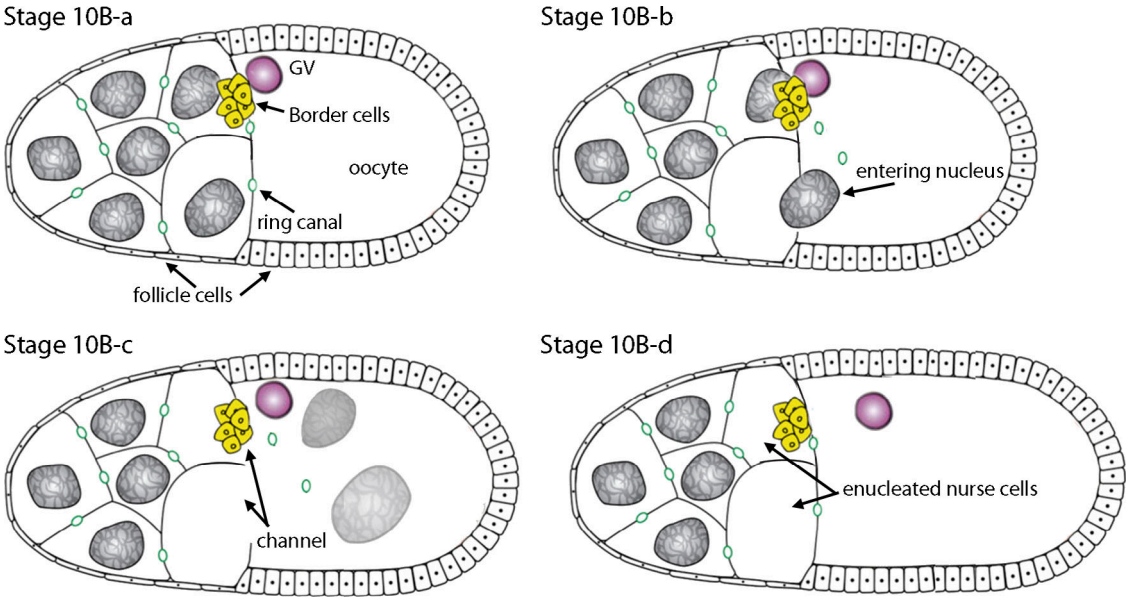

Figure 10. **NC nuclear elimination in stage 10B egg chambers.** Summary diagram illustrating the principal features of nuclear elimination. Subsequent to the anterodorsal localization of the GV (purple) in close proximity to the border cells (yellow; a), RCs (green) migrate into the oocyte and a pore forms that directly connects the oocyte with adjacent NCs (b), NCN translocate into the oocyte (c), and the GV migrates posteriorly (d). The NCN are absent from egg chambers in which the RCs have returned to the interface of the oocyte with enucleated NCs.

images in Fig. 1 C of Imran Alsous et al. (2021) show the ooplasm clearing associated with NC nuclear entry. Lastly, Drs. K. McCall and W. Sullivan have independently confirmed the presence of ectopic nuclei in stage 10B oocytes (personal communication). We conclude that there is significant support for our model in both published and unpublished data.

The next issue we address is the significance of NC enucleation. Although the NCN that enter the oocyte dissipate in the ooplasm, we do not consider it likely that they enter the oocyte to contribute nuclear components, because RCs provide direct conduits for NC products. Other possibilities are that these nuclei were programmed such that rapid elimination prevents them from making something deleterious, or that enucleation at stage 10B initiates a process that creates an efficient outlet for rapid transfer of materials from these NCs and from the NC compartment to the oocyte.

Stage 10B is a period when the growth rate of the oocyte increases from a doubling time of ∼5.5 h that does not appear to vary for stages 2 to 10A (Fig. 5 E). The doubling time of oocytes at stage 10B and subsequent stages that we measured is ∼2.8 h, a rate that is less than the 30 min reported previously (Guild et al., 1997), but that nonetheless would be a significant increase over the previous stages. The increased growth rate is consistent with the idea that stage 10B initiates the dumping period of rapid transport of NC components into the oocyte (Matova and Cooley, 2001). Dumping has been attributed to concerted "contraction" and "expulsion" through RCs that increase gradually in size throughout the earlier stages (Warn et al., 1985). However, the RCs of stage 10B egg chambers are ∼10 µm in diameter, much smaller than the NCN (∼30 µm in diameter) that enter the oocyte. We found that the NCN move into the oocyte through a large channel that directly connects NC cytoplasm with ooplasm; they do not move into the oocyte through RCs (Figs. 6, 7, and 8). The channel opens coincident with rapid dumping, and although we lack definitive evidence that the channel is present later in stages 12 and 13 egg chambers, we found evidence for its presence at stage 11. The RCs persist during these stages and presumably continue to provide a means for cytoplasm transfer, but the presence of a channel is consistent with the possibility that the channel is a second type of portal during the dumping period.

This potential role for the channel does not indicate why specific NCs become enucleated, but it is consistent with the phenotype of oocytes in egg chambers that do not reduce the number of NCN. Stages 12 and 13 egg chambers that retain 15 NCN are similar in size to stage 12–13 egg chambers with 13 NCN, but they have abnormal morphology (Fig. 9). It may be relevant that the number of NCN in stage 11 egg chambers varies: ∼60% have 13 NCN, ∼20% have 14, and ∼6% have 12, and the fraction of egg chambers that have 15 nucleated NCs is the same as the fraction of stage 11–13 oocytes that are morphologically abnormal. We suggest that oocyte maturation may proceed normally in egg chambers with 12, 13, and 14 nucleated NCs, but not in egg chambers that do not successfully create a channel to execute the nuclear extrusion process.

If this rationale for enucleation seems convoluted, the biology that enables it is fascinating and complex. For example, the cell fusion that joins the stage 10B oocyte with NCs is unique in several respects. First, it is prepatterned by the arrangement of the specified NCs that fuse with the oocyte. Second, its scale is massive due to the dimensions of the channel that joins the large oocyte and large NCs. Third, it appears to be reversible in the sense that the enucleated NCs of stage 11 egg chambers have shapes and appearances that are similar to their nucleated neighbors, despite the small opening that remains. Finally, the fusion-generated channel not only makes nuclear extrusion and

cytoplasmic mixing possible, but also brings the cluster of border cells, which are of somatic origin, and the GV of the oocyte into close proximity (Fig. 6, A–F). It is known both that the border cells move in a stereotyped sequence when they reach the anterior face of the oocyte and that failure to complete the sequence does not allow for normal oocyte maturation (Duchek and Rørth, 2001; Montell, 2003). However, the position of the border cells in the channel is a novel feature that raises the possibility of a role for the border cells in the enucleation program or, alternatively, a role for the cell fusion/enucleation program in bringing the GV and border cells together.

Our studies determined that the process of nuclear elimination does not require functions that mediate apoptosis such as cleaved caspase-3, but we did not identify the process that removes the NCN in the ooplasm. Our observations indicate that the process of enucleation differs from entosis, a phenomenon observed in cell cultures in which cells become internalized into neighboring cells and in which nuclei become condensed and fragmented (Overholtzer et al., 2007). In the *Drosophila* egg chamber, only NCN enter the oocyte, and the nuclei expand during the process of elimination. NC enucleation also lacks apparent similarities to erythroblast differentiation, which has been described as a type of asymmetric cell division in which the nucleus is extruded as a plasma membrane–encased body that is subsequently engulfed by a macrophage. In contrast to the nuclear elimination of the *Drosophila* NCs, cell fusion is not involved in erythroblast enucleation.

Fusion of NCs with a companion oocyte is a feature of oogenesis that has been observed in many animals, including mammals. This work provides unexpected and fascinating details of this process, as well as evidence that it may play an important role in egg maturation.

Materials and methods

Fly lines

The fly lines used were MTD-Gal4 (#31777; Bloomington), UAS-CD8:GFP (Roy et al., 2011), and Act5C-Gal4/CyO, Dpp:Cherry (Fereres et al., 2019).

Antibodies

The antibodies used in this study were mouse α-lamin, mouse α-HTS, and rat α-cadherin (Developmental Studies Hybridoma Bank); α-cleaved *Drosophila* DCP-1 (#9578; Cell Signaling Technology); α-MSP300 (Y. Gruenbaum, Department of Genetics, Institute of Life Sciences, Hebrew University of Jerusalem, Jerusalem, Israel), and mouse mAb 414 (M. D'Angelo, Development, Aging and Regeneration Program, Sanford Burnham Prebys Medical Discovery Institute, La Jolla, CA).

Histology

Antibody staining

5–10 pairs of ovaries were dissected in PBS together with their common duct, the linked ovaries were transferred with forceps to a watch glass with 16% formaldehyde, and after 5 min, the ovarioles were gently separated with fine forceps, transferred to an Eppendorf tube, and rotated slowly for 30 min, followed by at least three 10-min washes in PBT (PBS + 0.3% Triton X-100 + 0.1% Tween). Preparations were incubated in 5% normal donkey serum (NDS; 1 h, RT), washed once with PBT, and stained overnight with antibody together with 5% NDS. Stained embryos were washed three times for 15 min with PBT, incubated for 2 h with secondary antibody in PBT + NDS, and washed five times with PBT. All images were obtained with a Leica SPE confocal microscope.

Ovary preparation

"Normal" preparations were from flies 4–6 d after eclosion that had been incubated at 25°C in bottles (20–25 females and 15–20 males) and transferred to bottles with fresh medium 2–3 d before dissection. "Optimized" preparations were from flies (20–25 females and 15–20 males) 3 and 4 d after eclosion that had been transferred daily to fresh bottles supplemented with dry yeast.

Full ovary preparations (as in Fig. 1 A) were dissected in PBS, and several paired ovaries (linked by their common duct) were transferred with forceps to an Eppendorf tube with 16% formaldehyde for 30 min, washed 3 × 10 min with PBT, stained with DAPI (10 min), washed 3 × 10 min with PBT, and transferred by pipette to a microscope slide (one pair/slide). Liquid surrounding the ovary pair was removed with Kimwipe tissue and replaced with Vectashield mounting medium. Support, either a coverslip or layer of tape, was placed to either side of the ovaries, followed by a standard 1.5H coverslip, and sealed with nail polish.

Analysis of *D. simulans*, *D. hydei*, and *D. virilis* was of 40 ovaries for each species. Identified and recorded for *D. simulans*: 2 stage 10A/early 10B with 15 NCN, 7 late stage 10B with entering NCN, 3 stage 11 with 13 NCN, and 3 stage 12 with 13 NCN; for *D. hydei*: 2 late stage 10B with entering NCN and 5 stage 11 with 13 NCN; for *D. virilis*: 2 stage 9 with 15 NCN, 3 early-stage 10B with 15 NCN, 4 late stage 10B with entering NCN, 3 stage 11 with 13 NCN, and 1 stage 12 with 13 NCN.

Imaging live egg chambers

To view unfixed (live) preparations, ovaries were dissected from *MTD-Gal4/UASp-NLSGFP* females 3 d after eclosion in PBS or modified Schneider's medium (Peters and Berg, 2016) directly on a microscope slide. The outer sheath was disrupted with either a tungsten needle or fine forceps to free the ovarioles, supports were placed to either side, and a coverslip was placed over the preparation. For time-lapse imaging, ovaries were dissected in sterile modified Schneider's medium following the protocol described in Peters and Berg (2016). Ovaries were placed in a watch glass, and ovarioles were separated by gently severing the ovary sheath with a fine needle/forceps. A 6-mm-diameter well was generated by pouring 1% agarose into a 35-mm glass-bottom dish with the back of a pipette tip set in the middle of the dish. Agarose allows media permeation, while the well minimizes sample drifting caused by stage movement. Ovaries were transferred into a well filled with the culture medium and allowed to settle at the bottom of the dish. For fluorescence imaging, samples were placed on a single-objective light-sheet microscope, and a 3D volume with a field of view of 2 × 0.8 × 0.2 mm was acquired at 30-s intervals for 3.3 h. Objective lens: Olympus XLUMPLFLN20XW NA1.0, water. Excitation wavelength: 488 nm. Emission filter: Chroma ET525/

50. Technical details of the microscope can be found in Yang et al., 2021 *Preprint*).

To analyze NCN, fixed ovariole preparations from flies that express nuclear-localized GFP (MTD-Gal4>UASp-NLSGFP) were stained with antibody and mounted under a supported coverslip for imaging. Approximately 250 confocal optical sections separated by 0.27 µm were recorded, and the images were assembled with ImageJ to create a 3D rendering. To count NCN, the 3D structure was rotated to identify each nucleus in preparations that were stained with phalloidin to mark cell borders, and the number of RCs associated with each nucleus was determined. Each of the 16 germline cells has a unique signature composed of the number of RCs and nearest neighbors with 1, 2, 3, or 4 RCs.

Egg chamber volumes were determined by measuring the total length (L_{OC}), width (W), and depth (D) of DAPI-stained preparations and calculated by assuming an ellipsoid shape ($4/3 \times \pi \times L_{OC} \times D \times W$). Oocyte volumes were determined by measuring the length of the oocyte (L_O) and calculating the volume as $4/3 \times \pi \times L_O \times D \times W$. For each stage, $n \geq 10$.

To analyze egg chamber phenotypes, WT females 3 and 10 d after eclosion that had been transferred daily to bottles with fresh medium were stained with DAPI and imaged by confocal microscopy. 40 ovaries were analyzed for each time point. Egg chambers analyzed: 3 d, 96 stage 11–13 and 104 stage 14; and 10 d, 192 stage 11–13 and 152 stage 14. To analyze embryo phenotypes, 100 embryos from 4-h collections laid by WT females 3, 10, and <14 d (mixed) after eclosion were incubated for 18 h. Unhatched embryos were mounted directly in PBS on a microscope slide and imaged under a supported coverslip. Total unhatched embryos: mixed, 36/300 embryos; 3 d, 11/200 embryos; and 10 d, 66/300 embryos.

Ex vivo culture

Ovaries removed from females 3 d after eclosion were dissected in sterile modified Schneider's medium following the protocol described in Peters and Berg (2016). Ovaries were placed in a watch glass, and ovarioles were separated by gently severing the ovary sheath with a fine needle/forceps. Egg chambers were cultured at RT in a watch glass and viewed with a dissecting microscope and transmitted light. Midstage 10B egg chambers identified by the location of the GV were isolated and mounted for photography using a compound microscope, fixed for imaging with a confocal microscope, or incubated in situ for further development.

EM

Ovaries were removed from WT females under a dissecting microscope in PBS on a microscope slide set on an ice-chilled plate. The slide was transferred to a transmitted-light dissecting microscope, the ovary was gently disrupted to slightly separate ovarioles, and stage 10B egg chambers were identified. With the stage 10B egg chambers with oocytes that had slightly cleared, small regions near their anterior face were transferred with a cutoff Eppendorf pipette tip in a volume of 5 µl to immersion fixation consisting of either 2% glutaraldehyde in 0.1 M Na-cacodylate buffer, pH 7.3, for 1 h at RT or 1% glutaraldehyde/1% OsO_4 in 0.1 M Na-cacodylate buffer, pH 7.3, for 45 min on ice. After fixation, samples were rinsed in 0.1 M Na-cacodylate buffer, followed by postfixation in 1% OsO_4 in 0.1 M Na-cacodylate buffer for 1 h at RT. The samples were then rinsed with water and stained en bloc with 5% uranyl acetate in water for 1 h at RT. Following en bloc staining, the samples were rinsed with water, dehydrated in an ethanol series followed by propylene oxide, infiltrated, and then polymerized in Eponate 12 resin (Ted Pella). 50-nm sections were cut with a Leica UCT ultramicrotome (Leica Microsystems) using a diamond knife (Diatome USA), picked up on Pioloform-coated slot grids, and stained with uranyl acetate and Sato's lead (Sato, 1968). Sections were imaged with a FEI Tecnai 12 TEM at 120 kV using a Gatan 4k × 4k camera. TrakEM2 in Fiji was used to align image montages (Cardona et al., 2012; Schindelin et al., 2012).

Online supplemental material

Fig. S1 shows time-lapse fluorescence images of early stages of NC nuclear entry. Fig. S2 shows fine-structure images of ooplasm. Fig. S3 shows the NC:oocyte interface of a stage 11 egg chamber. Fig. S4 shows abnormal embryos with characteristics of egg chambers that do not eliminate NCN. Video 1 was generated from 221 consecutive (0.21-µm) optical sections of the early stage 10B egg chamber. Video 2 was generated from 76 consecutive (0.88-µm) optical sections of the stage 11 egg chamber. Video 3 shows an NC nucleus moving through a stage 10B oocyte. Table S1 shows frequencies of stage 10 egg chambers with entering nurse cell nuclei. Table S2 shows dimensions of stage 2–13 egg chambers and oocytes.

Acknowledgments

We thank W. Sullivan, S. Younger, and the Bloomington Stock Center for fly stocks; M. D'Angelo for mAb 414 antibody; Y. Gruenbaum for α-Msp300 antibody; and the Developmental Studies Hybridoma Bank for α-lamin, α-HTS, and α-cadherin antibodies.

This work was funded by National Institutes of Health grants R01GM109410 and R35GM122548 to T.B. Kornberg.

The authors declare no competing financial interests.

Author contributions: Z. Ali-Murthy: investigation; R.D. Fetter: investigation; W. Wang: investigation; B. Yang: investigation; L.A. Royer: methodology and supervision; T.B. Kornberg: conceptualization, methodology, writing – original draft, review, editing, supervision, project administration, funding acquisition.

Submitted: 17 December 2020
Revised: 11 March 2021
Accepted: 13 April 2021

References

Alexandrova, O., M. Schade, A. Böttger, and C.N. David. 2005. Oogenesis in Hydra: nurse cells transfer cytoplasm directly to the growing oocyte. *Dev. Biol.* 281:91–101. https://doi.org/10.1016/j.ydbio.2005.02.015

Baum, J.S., E. Arama, H. Steller, and K. McCall. 2007. The Drosophila caspases Strica and Dronc function redundantly in programmed cell death

during oogenesis. *Cell Death Differ.* 14:1508–1517. https://doi.org/10.1038/sj.cdd.4402155

Brown, E.H., and R.C. King. 1964. Studies on the events resulting in the formation of an egg chamber in Drosophila melanogaster. *Growth.* 28:41–81.

Cardona, A., S. Saalfeld, J. Schindelin, I. Arganda-Carreras, S. Preibisch, M. Longair, P. Tomancak, V. Hartenstein, and R.J. Douglas. 2012. TrakEM2 software for neural circuit reconstruction. *PLoS One.* 7:e38011. https://doi.org/10.1371/journal.pone.0038011

Chapman, R.F. 1999. The Insects. Cambridge University Press, Cambridge, UK.

Cummings, M.R., and R.C. King. 1969. The cytology of the vitellogenic stages of oogenesis in Drosophila melanogaster. *J. Morphol.* 128:427–441. https://doi.org/10.1002/jmor.1051280404

Cummings, M.R., and R.C. King. 1970. Ultrastructural changes in nurse and follicle cells during late stages of oogenesis in Drosophila melanogaster. *Z. Zellforsch. Mikrosk. Anat.* 110:1–8. https://doi.org/10.1007/BF00343981

Davis, L.I., and G. Blobel. 1986. Identification and characterization of a nuclear pore complex protein. *Cell.* 45:699–709. https://doi.org/10.1016/0092-8674(86)90784-1

de Cuevas, M., and A.C. Spradling. 1998. Morphogenesis of the Drosophila fusome and its implications for oocyte specification. *Development.* 125:2781–2789. https://doi.org/10.1242/dev.125.15.2781

Dej, K.J., and A.C. Spradling. 1999. The endocycle controls nurse cell polytene chromosome structure during Drosophila oogenesis. *Development.* 126:293–303. https://doi.org/10.1242/dev.126.2.293

Drummond-Barbosa, D., and A.C. Spradling. 2001. Stem cells and their progeny respond to nutritional changes during Drosophila oogenesis. *Dev. Biol.* 231:265–278. https://doi.org/10.1006/dbio.2000.0135

Duchek, P., and P. Rørth. 2001. Guidance of cell migration by EGF receptor signaling during Drosophila oogenesis. *Science.* 291:131–133. https://doi.org/10.1126/science.291.5501.131

Fereres, S., R. Hatori, M. Hatori, and T.B. Kornberg. 2019. Cytoneme-mediated signaling essential for tumorigenesis. *PLoS Genet.* 15:e1008415. https://doi.org/10.1371/journal.pgen.1008415

Foley, K., and L. Cooley. 1998. Apoptosis in late stage Drosophila nurse cells does not require genes within the H99 deficiency. *Development.* 125:1075–1082. https://doi.org/10.1242/dev.125.6.1075

Guild, G.M., P.S. Connelly, M.K. Shaw, and L.G. Tilney. 1997. Actin filament cables in Drosophila nurse cells are composed of modules that slide passively past one another during dumping. *J. Cell Biol.* 138:783–797. https://doi.org/10.1083/jcb.138.4.783

Huelsmann, S., J. Ylänne, and N.H. Brown. 2013. Filopodia-like actin cables position nuclei in association with perinuclear actin in Drosophila nurse cells. *Dev. Cell.* 26:604–615. https://doi.org/10.1016/j.devcel.2013.08.014

Imran Alsous, J., N. Romeo, J.A. Jackson, F.M. Mason, J. Dunkel, and A.C. Martin. 2021. Dynamics of hydraulic and contractile wave-mediated fluid transport during *Drosophila* oogenesis. *Proc. Natl. Acad. Sci. USA.* 118:e2019749118. https://doi.org/10.1073/pnas.2019749118

Imran Alsous, J., P. Villoutreix, A.M. Berezhkovskii, and S.Y. Shvartsman. 2017. Collective Growth in a Small Cell Network. *Curr. Biol.* 27:2670–2676.e4. https://doi.org/10.1016/j.cub.2017.07.038

Isasti-Sanchez, J., F. Münz-Zeise, and S. Luschnig. 2020. Transient opening of tricellular vertices controls paracellular transport through the follicle epithelium during Drosophila oogenesis. *BioRxiv*. (Preprint posted February 29, 2020) https://doi.org/10.1101/2020.02.29.971168

Jacob, J., and J.L. Sirlin. 1959. Cell function in the ovary of Drosophila. I. DNA classes in nurse cell nuclei as determined by autoradiography. *Chromosoma.* 10:210–228. https://doi.org/10.1007/BF00396572

King, R.C., A.C. Rubinson, and R.F. Smith. 1956. Oogenesis in adult Drosophila melanogaster. *Growth.* 20:121–157.

Koch, E.A., and R.C. King. 1966. The origin and early differentiation of the egg chamber of Drosophila melanogaster. *J. Morphol.* 119:283–303. https://doi.org/10.1002/jmor.1051190303

Lei, L., and A.C. Spradling. 2016. Mouse oocytes differentiate through organelle enrichment from sister cyst germ cells. *Science.* 352:95–99. https://doi.org/10.1126/science.aad2156

Matova, N., and L. Cooley. 2001. Comparative aspects of animal oogenesis. *Dev. Biol.* 231:291–320. https://doi.org/10.1006/dbio.2000.0120

Meier, E., B.R. Miller, and D.J. Forbes. 1995. Nuclear pore complex assembly studied with a biochemical assay for annulate lamellae formation. *J. Cell Biol.* 129:1459–1472. https://doi.org/10.1083/jcb.129.6.1459

Miller, M.A., U. Technau, K.M. Smith, and R.E. Steele. 2000. Oocyte development in Hydra involves selection from competent precursor cells. *Dev. Biol.* 224:326–338. https://doi.org/10.1006/dbio.2000.9790

Montell, D.J. 2003. Border-cell migration: the race is on. *Nat. Rev. Mol. Cell Biol.* 4:13–24. https://doi.org/10.1038/nrm1006

Overholtzer, M., A.A. Mailleux, G. Mouneimne, G. Normand, S.J. Schnitt, R.W. King, E.S. Cibas, and J.S. Brugge. 2007. A nonapoptotic cell death process, entosis, that occurs by cell-in-cell invasion. *Cell.* 131:966–979. https://doi.org/10.1016/j.cell.2007.10.040

Peters, N.C., and C.A. Berg. 2016. In Vitro Culturing and Live Imaging of Drosophila Egg Chambers: A History and Adaptable Method. *Methods Mol. Biol.* 1457:35–68. https://doi.org/10.1007/978-1-4939-3795-0_4

Peterson, J.S., and K. McCall. 2013. Combined inhibition of autophagy and caspases fails to prevent developmental nurse cell death in the Drosophila melanogaster ovary. *PLoS One.* 8:e76046. https://doi.org/10.1371/journal.pone.0076046

Peterson, J.S., M. Barkett, and K. McCall. 2003. Stage-specific regulation of caspase activity in drosophila oogenesis. *Dev. Biol.* 260:113–123. https://doi.org/10.1016/S0012-1606(03)00240-9

Prasad, M., A.C.-C. Jang, M. Starz-Gaiano, M. Melani, and D.J. Montell. 2007. A protocol for culturing Drosophila melanogaster stage 9 egg chambers for live imaging. *Nat. Protoc.* 2:2467–2473. https://doi.org/10.1038/nprot.2007.363

Roy, S., F. Hsiung, and T.B. Kornberg. 2011. Specificity of Drosophila cytonemes for distinct signaling pathways. *Science.* 332:354–358. https://doi.org/10.1126/science.1198949

Sato, T. 1968. A modified method for lead staining of thin sections. *J. Electron Microsc. (Tokyo).* 17:158–159.

Schindelin, J., I. Arganda-Carreras, E. Frise, V. Kaynig, M. Longair, T. Pietzsch, S. Preibisch, C. Rueden, S. Saalfeld, B. Schmid, et al. 2012. Fiji: an open-source platform for biological-image analysis. *Nat. Methods.* 9:676–682. https://doi.org/10.1038/nmeth.2019

Spracklen, A.J., and T.L. Tootle. 2013. The utility of stage-specific mid-to-late Drosophila follicle isolation. *J. Vis. Exp.* (82):50493. https://doi.org/10.3791/50493

Spradling, A.C. 1993. Developmental genetics of oogenesis. *In* The development of Drosophila melanogaster. Bate, M., ed. Cold Spring Harbor Press, Cold Spring Harbor, NY; 1–70.

Warn, R.M., H.O. Gutzeit, L. Smith, and A. Warn. 1985. F-actin rings are associated with the ring canals of the Drosophila egg chamber. *Exp. Cell Res.* 157:355–363. https://doi.org/10.1016/0014-4827(85)90120-X

Xue, F., and L. Cooley. 1993. kelch encodes a component of intercellular bridges in Drosophila egg chambers. *Cell.* 72:681–693. https://doi.org/10.1016/0092-8674(93)90397-9

Yang, B., M. Lange, A. Millett-Sikking, A.C. Solak, S.V. Kumar, W. Wang, H. Kobayashi, M.N. McCarroll, L.W. Whitehead, R.P. Fiolka, et al. 2021. High-Resolution, Large Imaging Volume, and Multi-View Single Objective Light-Sheet Microscopy. *bioRxiv*. (Preprint posted April 19, 2021) https://doi.org/10.1101/2020.09.22.309229

Zimmerman, S.G., G.E. Merrihew, M.J. MacCoss, and C.A. Berg. 2017. Proteomics Analysis Identifies Orthologs of Human Chitinase-Like Proteins as Inducers of Tube Morphogenesis Defects in *Drosophila melanogaster*. *Genetics.* 206:973–984. https://doi.org/10.1534/genetics.116.199323

Supplemental material

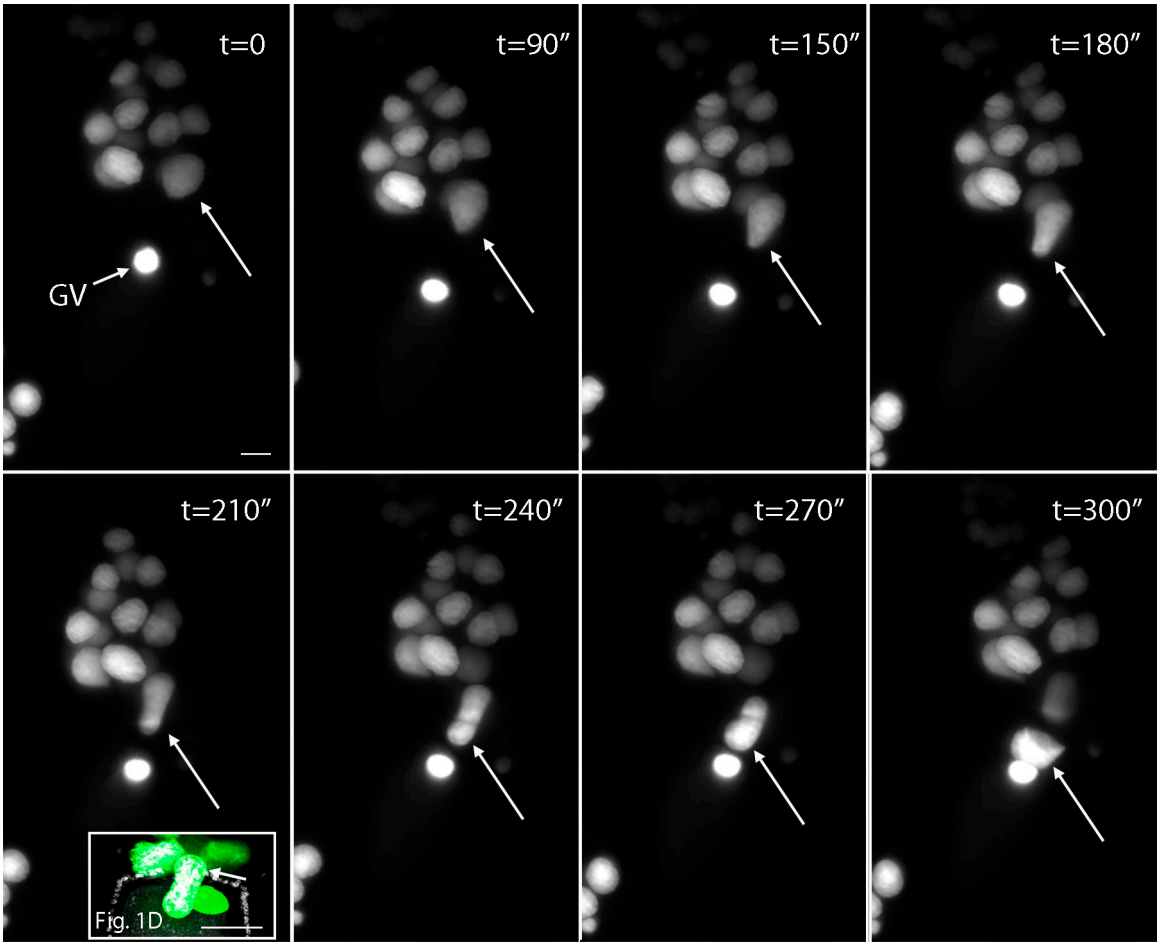

Figure S1. **Frames from time-lapse fluorescence images of the early stages of NC nuclear entry captured by lattice light sheet microscopy.** Arrows indicate the entering NC nucleus. Inset from Fig. 1 D shows similar shapes of the entering NCN in the live fluorescence image (time 240 min) and after fixation. Scale bars: 50 µm.

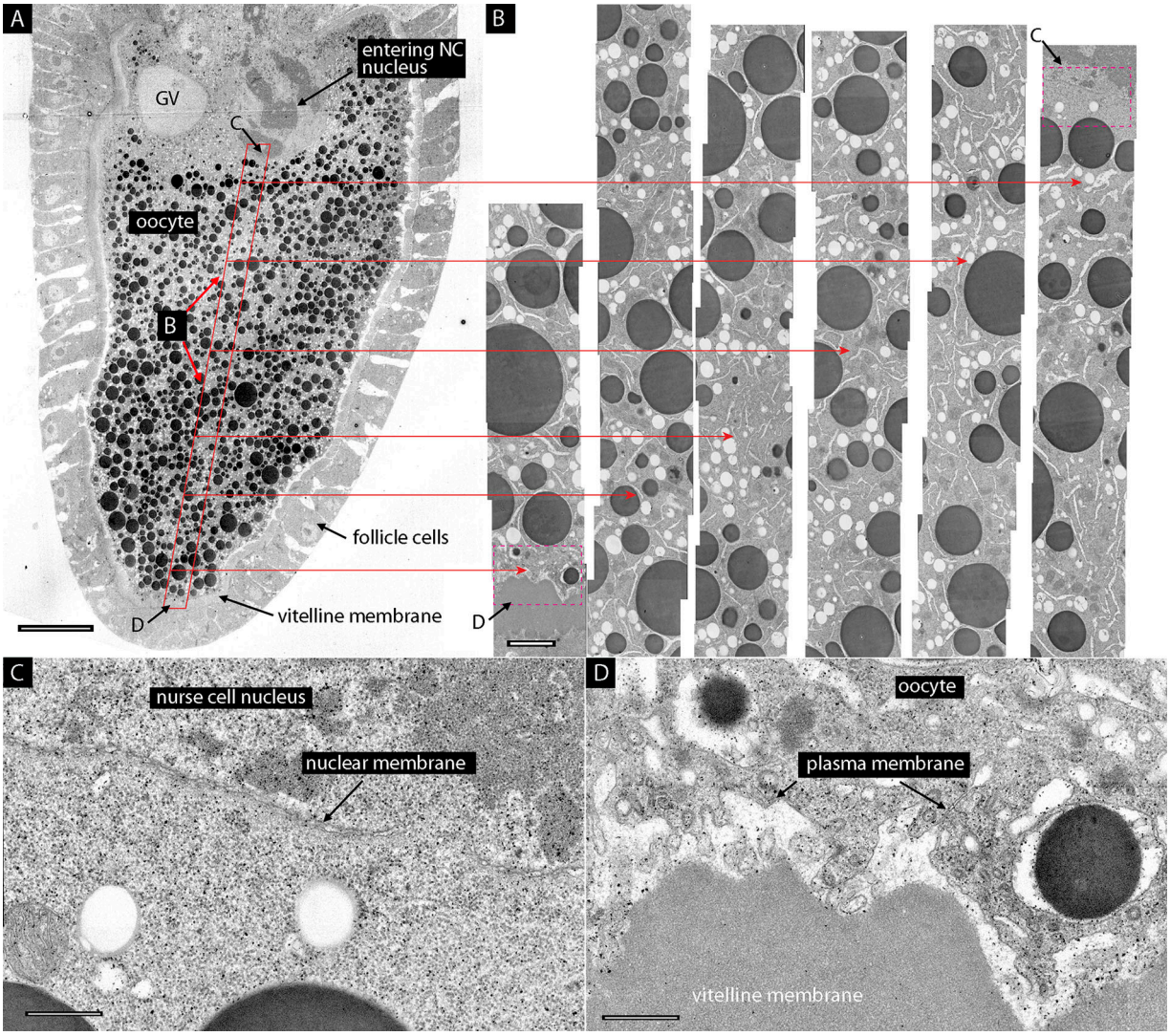

Figure S2. **Fine-structure images of ooplasm. (A and B)** EM of a stage 10B egg chamber with an entering NC nucleus showing the oocyte at low magnification (A) and a montage of high-magnification images (B) showing the ooplasm devoid of membrane between the entering NC nucleus at the anterior and plasma oocyte membrane juxtaposed to vitelline membrane at the posterior pole. **(C and D)** Fine structure of the nuclear membrane of the entering NC (C) and oocyte plasma membrane (D). Scale bars: 20 µm (A and B); 5 µm (C and D).

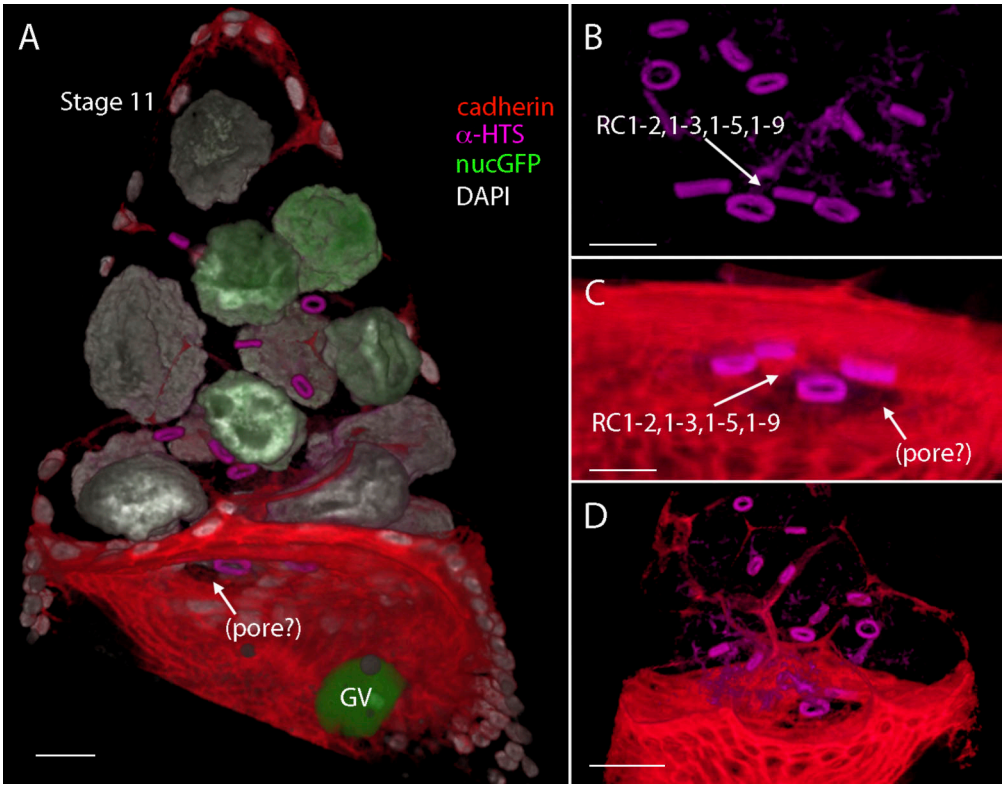

Figure S3. **Images from a 3D reconstruction of a stage 11 egg chamber that expressed nucGFP and was stained with DAPI and with antibodies against cadherin and HTS. (A–D)** The RCs that connect the oocyte with NCs are visible at the surface of the anterior face of the oocyte (A–C), but these images did not resolve whether the apparent discontinuity of cadherin staining in this region (A, C, and D) was due to the presence of a channel or to the complex morphology. Scale bars: 50 µm.

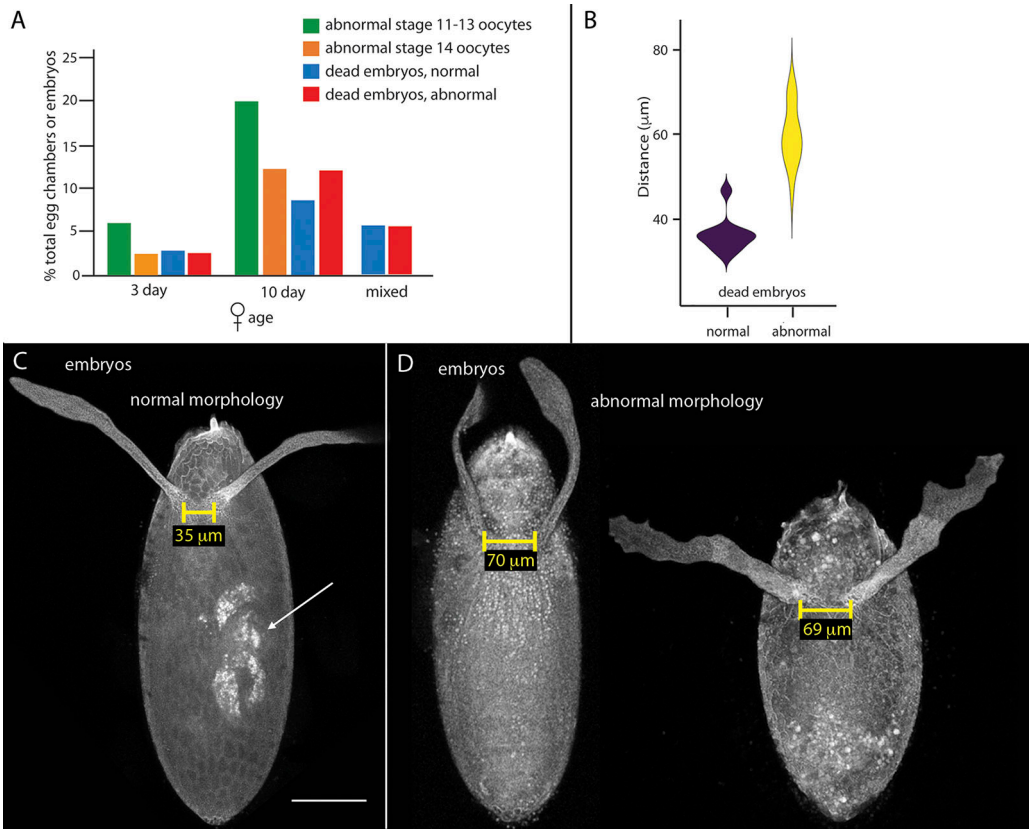

Figure S4. **Nondeveloping embryos with abnormalities characteristic of egg chambers that do not eliminate NCN. (A)** Graph indicating percentage of stage 11–13 and stage 14 egg chambers with abnormal morphology laid by 3- and 10-d-old females, and percentage of unhatched embryos laid by females of mixed age, 3 and 10 d after eclosion with normal or abnormal morphology. **(B)** Violin plot showing distributions of distances between dorsal appendages of inviable embryos that either developed to organogenesis stages (normal) or appeared to be unfertilized (abnormal). **(C and D)** Embryos with normal (C) and abnormal (D) morphology, with distance between developing dorsal appendages marked and autofluorescent internal organs indicated by arrow. Scale bar: 100 µm (bar in C for C and D).

Video 1. **Video generated from 221 consecutive (0.21-µm) optical sections of the early stage 10B egg chamber.**

Video 2. **Video generated from 76 consecutive (0.88-µm) optical sections of the stage 11 egg chamber.**

Video 3. **Video generated from photographs taken at 1-min intervals as described in Materials and methods and played at 2 frames/s.** White arrow, approximate location of NC nucleus entry; yellow arrows in frames 8–28, clearing in the ooplasm caused by the presence of the NC nucleus.

Provided online are two tables. Table S1 shows frequencies of stage 10 egg chambers with entering nurse cell nuclei. Table S2 shows dimensions of stage 2–13 egg chambers and oocytes.